

Hydrological Changes in Restricted Basins: Insights From Strontium Isotopes on Late Miocene-Pliocene Connectivity of the Eastern Paratethys (Dacian Basin, Romania)

Iuliana Vasiliev, Marius Stoica, Arjen Grothe, Sergei Lazarev, Dan Valentin Palcu, Christiaan van Baak, Arjan de Leeuw, Francesca Sangiorgi, Gert-Jan Reichart, Gareth R. Davies, et al.

▶ **To cite this version:**

Iuliana Vasiliev, Marius Stoica, Arjen Grothe, Sergei Lazarev, Dan Valentin Palcu, et al.. Hydrological Changes in Restricted Basins: Insights From Strontium Isotopes on Late Miocene-Pliocene Connectivity of the Eastern Paratethys (Dacian Basin, Romania). Geochemistry, Geophysics, Geosystems, 2021, 22, 10.1029/2020GC009369 . insu-03691312

HAL Id: insu-03691312
https://insu.hal.science/insu-03691312

Submitted on 9 Jun 2022

HAL is a multi-disciplinary open access archive for the deposit and dissemination of scientific research documents, whether they are published or not. The documents may come from teaching and research institutions in France or abroad, or from public or private research centers.

L'archive ouverte pluridisciplinaire **HAL**, est destinée au dépôt et à la diffusion de documents scientifiques de niveau recherche, publiés ou non, émanant des établissements d'enseignement et de recherche français ou étrangers, des laboratoires publics ou privés.



Distributed under a Creative Commons Attribution - NoDerivatives 4.0 International License

Check for updates

Geochemistry, Geophysics, Geosystems

RESEARCH ARTICLE
10.1029/2020GC009369

Key Points:

- The early Maeotian transgression (7.6–7.4 Ma) started with an incursion of Eastern Paratethys (i.e., Black Sea) waters into the Dacian Basin
- The Maeotian-Pontian transition (6.3–5.9 Ma) records a second incursion of Eastern Paratethys followed by a short influx of marine (Mediterranean) waters
- The Bosphorian transgression at ca. 5.5 Ma was probably related to the increased influence of Pannonian and local river water in the Dacian Basin

Correspondence to:
I. Vasiliev,
Iuliana.Vasiliev-Popa@senckenberg.de;
iuli.iuliana@yahoo.com

Citation:
Vasiliev, I., Stoica, M., Grothe, A., Lazarev, S., Palcu, D. V., van Baak, C., et al. (2021). Hydrological changes in restricted basins: Insights from strontium isotopes on late Miocene-Pliocene connectivity of the Eastern Paratethys (Dacian Basin, Romania). *Geochemistry, Geophysics, Geosystems*, *22*, e2020GC009369. https://doi.org/10.1029/2020GC009369

Received 10 AUG 2020
Accepted 5 MAR 2021

© 2021. The Authors.
This is an open access article under the terms of the Creative Commons Attribution License, which permits use, distribution and reproduction in any medium, provided the original work is properly cited.

Hydrological Changes in Restricted Basins: Insights From Strontium Isotopes on Late Miocene-Pliocene Connectivity of the Eastern Paratethys (Dacian Basin, Romania)

Iuliana Vasiliev[1,2], Marius Stoica[2], Arjen Grothe[3], Sergei Lazarev[3], Dan Valentin Palcu[3,4], Christiaan van Baak[3,5], Arjan De Leeuw[6], Francesca Sangiorgi[3], Gert-Jan Reichart[3,7], Gareth R. Davies[8], and Wout Krijgsman[3]

[1]Senckenberg Biodiversity and Climate Research Centre (SBiK-F), Frankfurt am Main, Germany, [2]Department of Geology, Bucharest University, Bucharest, Romania, [3]Department of Earth Sciences, Utrecht University, Utrecht, The Netherlands, [4]Oceanographic Institute of the University of Sao Paulo, Sao Paulo, Brazil, [5]CASP, Cambridge, UK, [6]Institut des Sciences de la Terre, Université Grenoble Alpes, Grenoble, France, [7]Royal Netherlands Institute for Sea Research (NIOZ), Texel, The Netherlands, [8]Geology & Geochemistry, VU University, Amsterdam, The Netherlands

Abstract The Dacian Basin was uniquely situated to record late Miocene hydrological changes that influenced depositional environments and faunal dispersal patterns in Central Eurasia's mega-lake Paratethys. Differences between the high strontium isotope ratio ($^{87}Sr/^{86}Sr$) of the waters from Lake Pannon and local Carpathian rivers and low $^{87}Sr/^{86}Sr$ of the Eastern Paratethys (Black Sea – Caspian Sea) allow a thorough investigation of connectivity and water fluxes in the transient Dacian Basin. We present a detailed $^{87}Sr/^{86}Sr$ record for the Dacian Basin, which provides an exceptional record of basin connectivity from the latest Tortonian (ca. 7.7 Ma) until the early Pleistocene (ca. 1.8 Ma). Data show that a late Tortonian transgression (7.6–7.4 Ma) started with an incursion of Eastern Paratethys waters into the Dacian Basin, after which local rivers became the dominant source for the mostly freshwater environments of the early Messinian. The regional Maeotian-Pontian transitional interval (6.3–5.9 Ma) records a second incursion of Eastern Paratethys waters, but this time with an additional marine (Mediterranean) influx coinciding with a short-lived salinity incursion. During the Messinian Salinity Crisis of the Mediterranean, the Dacian Basin progressively connected with the Eastern Paratethys (5.9–5.5 Ma), after which it became restricted during the peak Mediterranean lowstand (5.5 Ma) and filled with Lake Pannon and local river water (5.5–5.3 Ma). During the Plio-Pleistocene, the Dacian Basin reconnected with the, at that time isolated, Black Sea, which shows similar $^{87}Sr/^{86}Sr$ as in the Last Glacial Maximum.

Plain Language Summary The late Miocene Dacian Basin (western appendix of the Black Sea) was uniquely situated to record hydrological changes that influenced environments and faunal dispersal patterns in Central Eurasia's mega-lake Paratethys. We used strontium isotopes from the Dacian Basin to track the moments of changing connections with Paratethys and the open ocean, via the Mediterranean. We found that at 7.6–7.4 Ma, an invasion of Eastern Paratethys waters provoked the so-called Maeotian transgression. Afterward local rivers became the dominant source for the mostly freshwater environments, interrupted at 6.1 Ma by an influx of marine, salty water from Mediterranean. During the Messinian Salinity Crisis (5.9–5.3 Ma), when the Mediterranean suffered from an interrupted connectivity to the Atlantic Ocean, the Dacian Basin progressively connected with the Eastern Paratethys (Black Sea and Caspian Sea). At the peak of Messinian Salinity Crisis in the Mediterranean (5.5 Ma), the Dacian Basin became restricted and filled with Lake Pannon and local river water (5.5–5.3 Ma). During the Plio-Pleistocene (between 5.3 and 1.8 Ma), the Dacian Basin reconnected with the, at that time isolated, Black Sea, providing a situation similar to the one during the Last Glacial Maximum.

1. Introduction

Semi-isolated basins like the Black Sea and the Mediterranean are highly sensitive to changes in connectivity, which directly influence basin-wide paleoenvironmental conditions (i.e., salinity, temperature, nutrients)

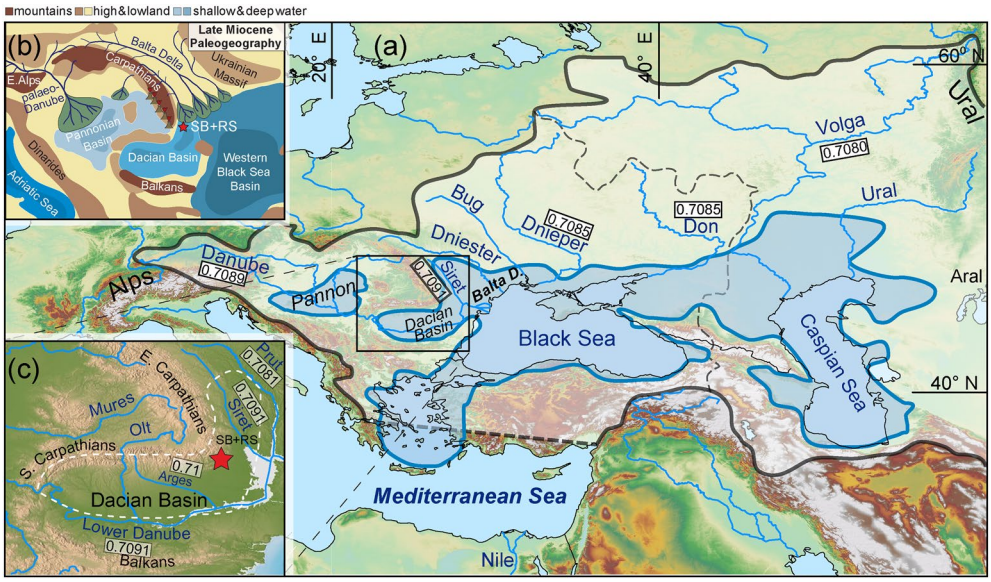


Figure 1. (a) Elevation map showing the extent of the Paratethys during the early Pontian (blue solid line surrounding pale blue shading). The four main sub-basins are, from west to east: Pannonian Basin, Dacian Basin, Black Sea (Euxinic) Basin and the Caspian Basin. The present-day catchments of these basins are outlined by a thick dark gray line. The present-day $^{87}Sr/^{86}Sr$ of the main rivers are indicated in white boxes (Clauer et al., 2000; Palmer & Edmond, 1992; Zitek et al., 2015); (b) Paleogeography of Dacian Basin and adjacent basins (modified after De Leeuw et al., 2020) during late Miocene. Balta Delta covered largely overlapped the present-day Dniester, Prut, southern Bug and Siret rivers; (c) Inset depicts a close-up of the Dacian Basin showing the studied sections (SB = Slanicul de Buzau, RS = Rîmnicu Sărat) and important rivers that are descendants of the former rivers draining into the Dacian Basin.

(e.g., Bethoux and Pierre, 1999; Cramp and O'Sullivan, 1999; Karami et al., 2011; Simon et al., 2019) and determine faunal dispersals (e.g., Stoica et al., 2016; Grothe et al., 2018; Lazarev et al., 2020). The most dramatic expressions of changes in water exchange are the so-called salinity crises where evaporites form at times of restricted basin connectivity in regions with negative hydrological budgets. A key example is the Messinian Salinity Crisis (MSC; 5.97–5.33 Ma), which developed in the late Miocene Mediterranean Basin (e.g., Roveri, Flecker, et al., 2014) as a consequence of Atlantic–Mediterranean gateway restriction (e.g., Flecker et al., 2015; Krijgsman et al., 2018). Basin connectivity with the contemporary Paratethys (former Black Sea–Caspian Sea region; Figure 1) may also have played an important role in the MSC, as this Central Eurasian mega-lake potentially provided SO_4^{2-}-rich water (favoring gypsum formation) to the Mediterranean (Grothe et al., 2020).

In restricted basins, radiogenic strontium isotope ratios ($^{87}Sr/^{86}Sr$) can be a powerful tool to discriminate between the various sources of water (Flecker et al., 2002; Flecker & Ellam, 2006; Topper et al., 2011; Vonhof et al. 2003) and to infer phases of isolation or interbasinal connectivity (e.g., McCulloch & De Deckker, 1989). The $^{87}Sr/^{86}Sr$ of such basins are frequently offset from coeval ocean water signatures and controlled by mixing with regional strontium sources such as river water (Reghizzi et al., 2017, 2018; Roveri, Lugli, et al., 2014). A well-studied example is provided by the Mediterranean basin that recorded a marked transition from marine (at the onset of MSC at 5.97 Ma) to restrictive river dominated $^{87}Sr/^{86}Sr$ values (between 5.55 and 5.33 Ma), controlled by the increasing relative contribution of riverine versus marine water supply (e.g., Flecker et al., 2002; Roveri, Lugli et al., 2014; Schildgen et al., 2014; Reghizzi et al., 2018). Rivers generally have characteristic isotopic compositions and concentrations reflecting the lithology of the hinterland (e.g., Grothe et al., 2020; Andreetto, Matsubara et al., 2021). In the semi-isolated Paratethys, several isotopically different water sources contributed to its hydrology (e.g., proto-Danube, Don, Dnjepr, Volga, and intermittently the Mediterranean). During the MSC, Paratethys showed $^{87}Sr/^{86}Sr$ of 0.7084–0.7085 which are significantly below the coeval open ocean curve (0.7091–0.7092) but slightly higher than a fully isolated but interconnected basin system (0.7083) (Grothe et al., 2020). Mass balance models for the Paratethys suggest that an additional Mediterranean source of only ~4–10% of present-day marine input is required to explain the observed values.

A major complication in assessing the role of Paratethys on the MSC is that it consists of multiple sub-basins (Pannonian, Dacian, Black Sea, and Caspian basins), which are separated from each other by shallow sills (e.g., Van Baak et al., 2017). Minor variations in water level may therefore cause large changes in intra-basin connectivity. In such restricted basins, the local rivers play an important role on the hydrology and strongly influence $^{87}Sr/^{86}Sr$. Connectivity to marine domains, that have ca. 40 times higher strontium concentrations than rivers, would rapidly shift the $^{87}Sr/^{86}Sr$ signature in restricted basins to marine values (e.g., Grothe et al., 2020; Major et al., 2006; Yanchilina et al., 2019). The Dacian Basin of Romania is well situated to study connectivity changes in a restricted basin, because its local rivers (proto-Danube, Olt, southern Bug) have distinctly higher $^{87}Sr/^{86}Sr$ than the neighboring Eastern Paratethys domain, the epicontinental sea that covered vast parts of south eastern Eurasia with its renowned Black Sea and Caspian Sea remnants (Figure 1). Late Miocene $^{87}Sr/^{86}Sr$ data from the Dacian Basin (Vasiliev et al., 2010) are significantly higher (ca. 0.7089) than the Black and Caspian Seas (ca. 0.7085) at the same time (Grothe et al., 2020). This is remarkable, because the late Miocene (Pontian regional stage) is well-known as a period of aquatic faunal exchange across the entire Paratethys region (Popov et al., 2006; Stevanovic et al., 1989; Van Baak et al., 2017).

The main goal of our study is to improve understanding of the hydrology and connectivity of the Dacian Basin during the late Miocene and Pliocene by providing a high temporal resolution record of its $^{87}Sr/^{86}Sr$. Strontium isotope measurements on ostracod shells are reported as a geochemical proxy that allows a quantitative comparison between basins, irrespective of species compositions (Chivas et al., 1985). Due to its geographical position, the Dacian Basin forms the link between the Central (Pannonian Basin; Hungary) and Eastern Paratethys (Figure 1). From a paleoecological perspective, the Dacian Basin plays a vital role in the introduction of typical Pannonian (mollusk, ostracod and dinoflagellate) species into the Eastern Paratethys during the Maeotian and Pontian regional stages (Grothe et al., 2018), and later into the Mediterranean during the final phase of the MSC (Andreetto, Aloisi et al., 2021; Gliozzi et al., 2007; Stoica et al., 2016). The $^{87}Sr/^{86}Sr$ record of the Dacian Basin is of particular interest because the sedimentary infill of the basin is well studied and records multiple and complex connectivity events (Krijgsman et al., 2010; Lazarev et al., 2020; Marunţeanu and Papaianopol, 1995; Munteanu et al., 2012; Palcu et al., 2019; Stevanovic et al., 1989; Stoica et al., 2013). Ultimately, the $^{87}Sr/^{86}Sr$ presented here shed light on (a) the significance and mechanism of the Maeotian, lower Pontian, and Bosphorian transgressions in the Dacian Basin; (b) the connectivity of the Dacian Basin and Eastern Paratethys during the MSC; (c) the presence or absence of marine influences in Paratethys during the Zanclean flooding of the Mediterranean at 5.33 Ma.

2. Local Riverine Strontium Sources of the Dacian Basin

The Miocene Dacian Basin was a restricted foreland basin strongly affected by riverine inputs associated with the formation of the Carpathian Mountains (Jipa et al., 2009; Maţenco et al., 2003). The Danube River did not yet exist (De Leeuw et al., 2018; Magyar et al., 2019; Olariu et al., 2018), and the proto-Danube drained into Lake Pannon (Figure 1; Magyar et al., 1999; Magyar & Geary 2012). To the northeast of the Dacian Basin, the Balta Delta was fed by a major river system, significantly bigger than today (De Leeuw et al., 2020; Matoshko et al., 2016) and to a large degree sourced from the external Carpathians, in analogy with the present-day Dniester, Prut, southern Bug and Siret rivers (Figure 1). The $^{87}Sr/^{86}Sr$ of the Dacian Basin was therefore mainly determined by a combination of Pannonian outflow waters, drainage from the Carpathian Mountains (e.g., Arges, Prut, southern Bug, Siret rivers) and the inflow of anomalohaline waters via the Black Sea.

The present-day $^{87}Sr/^{86}Sr$ of the Danube, the main river in central Europe that flows from Southern Germany towards the Black Sea, is estimated between 0.7089 (Palmer and Edmond, 1992) and ca. 0.7091 (Zitek et al., 2015). The latter ratio is derived from an extensive study during which Danube water was sampled along its entire course, hence encompassing the full range of ratios associated with its drainage basin (Zitek et al., 2015). The lowest $^{87}Sr/^{86}Sr$ are encountered in the upstream part, where the Danube drains predominantly Mesozoic carbonates and Cenozoic sediments of the Alpine molasses (Pawellekl et al., 2002). The Mio-Pliocene catchment of the Pannonian Basin was roughly similar to present-day, but extended further to the north and west, including areas currently drained by for example, the Alpine Rhine and the Upper Main (Kuhlemann, 2007; Miklos & Neppel, 2010). A larger drainage basin may have decreased the strontium isotope ratio of the proto-Danube, because the catchments of the Alpine Rhine and the Main

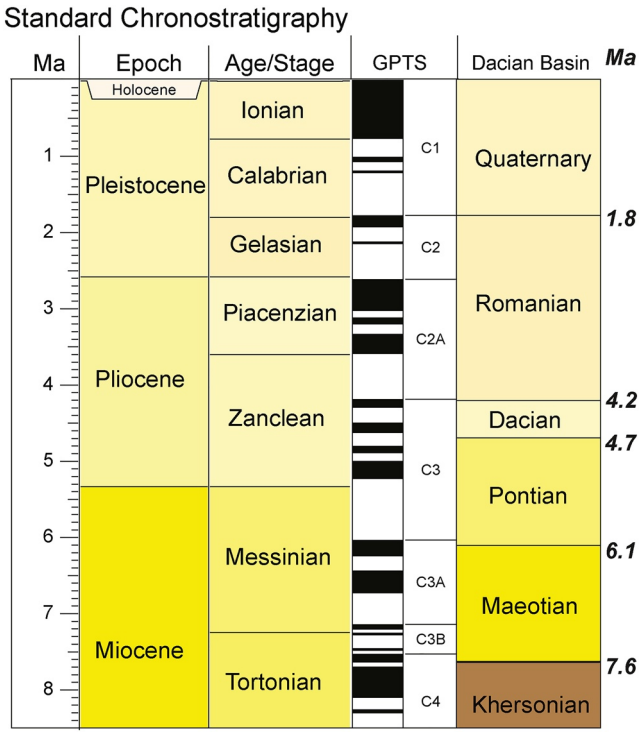


Figure 2. Stages used in the Dacian Basin part of the Paratethys and correlation to the standard time scale of Hilgen et al. (2012). The ages of the Dacian Basin stages, in million years, are according to van Baak, Mandic, et al. (2015), Palcu et al. (2019) and Lazarev et al. (2020).

are currently characterized by lower $^{87}Sr/^{86}Sr$: ca. 0.7085–0.7088 (Buhl et al., 1991; Kober et al., 2007). It has also been suggested, however, that the late Miocene Danube drained a larger part of the Bohemian Massif as well (Miklos & Neppel, 2010). This block is composed of Precambrian and Paleozoic igneous and metamorphic rocks, which are characterized by relatively high $^{87}Sr/^{86}Sr$ (Pawellekl et al., 2002). For example, the Morava River, an important tributary of the Danube draining part of the Bohemian Massif, has an $^{87}Sr/^{86}Sr$ of ca. 0.711 (Zitek et al., 2015), significantly higher than the Danube ratios of 0.7089–0.7091 (Palmer & Edmond, 1992; Zitek et al., 2015). Consequently, the Danube's $^{87}Sr/^{86}Sr$ increases to 0.7092–0.7093 after the confluence with the Morava River (Zitek et al., 2015). Considering the opposing effect of relative high $^{87}Sr/^{86}Sr$ of the Bohemian Massif and the relatively low $^{87}Sr/^{86}Sr$ of the Alpine Rhine, we assume the strontium isotope ratio of the Lake Pannon outflow waters to have been roughly similar to the present-day Danube: 0.7089–0.7091 (Palmer & Edmond, 1992; Zitek et al., 2015).

River water draining the Eastern Carpathians also sourced the Dacian Basin (De Leeuw et al., 2020; Jorissen et al., 2018; Lazarev et al., 2020; Panaiotu et al., 2007). Most of the Eastern Carpathians is composed of Jurassic, Cretaceous and Paleogene flysh-type deposits (Motas et al., 1966). The $^{87}Sr/^{86}Sr$ of rivers draining these areas is expected to be roughly similar to the $^{87}Sr/^{86}Sr$ of the Danube. This is confirmed by the Siret River, a small tributary of the Danube that drains a large portion of the East Carpathians (Figure 1), which has a strontium isotope ratio of ca. 0.7091 (Zitek et al., 2015). In contrast, the Southern Carpathians also contain Paleozoic rocks. The strontium isotope ratio of the Arges River, which drains the Southern Carpathians, is therefore, higher: ca. 0.710 (Zitek et al., 2015).

In summary, the strontium isotope ratio of the local fresh-water sources draining into the late Miocene Dacian Basin is considered relatively stable around 0.7091 (Zitek et al., 2015). The inflows of tributaries that bear water with significantly different $^{87}Sr/^{86}Sr$ have minimal effects on the strontium isotope ratio of the main rivers. We therefore consider that any large shift in the strontium isotope record of the Dacian Basin was not caused by changes in drainage but by connectivity changes with the Eastern Paratethys basins and/or the marine Mediterranean. Marine waters typically have strontium concentrations that are ca. 40 times higher than average global river water (Palmer & Edmond, 1992). Consequently, the $^{87}Sr/^{86}Sr$ of a restricted basin can be severely affected by relatively limited marine influence (Vonhof et al., 2003). It should be noted, however, that the strontium concentration of water from Lake Pannon and the Eastern Paratethys may have been much higher than present-day strontium concentrations of river water as these basins acted as isolated lake systems for about 6 Myr (Magyar et al., 1999; Popov et al., 2006) and basin water strontium concentrations could have increased over time.

3. Slanicul de Buzau Section

A variety of regional stages has been developed throughout the Paratethys because its unique, non-marine fauna does not allow for direct correlation to the open ocean record. The studied sedimentary succession along the Slanicul de Buzau river of the Dacian Basin comprises the Khersonian, Maeotian, Pontian, Dacian and Romanian regional stages (Figure 2). The Pontian Stage of the Dacian Basin is further divided into three substages (the Odessian, Portaferrian and Bosphorian) defined on the basis of macro and microfossils (mollusks, ostracods).

During the Khersonian, the water level in the Dacian Basin was relatively low and reflected by delta progradation (De Leeuw et al., 2020; Matoshko et al., 2016) and coastal plains with reddish palaeosols (Lazarev

et al., 2020; Palcu et al., 2019). The Maeotian transgression terminated the Khersonian, an event dated in Slanicul de Buzau at 7.63 Ma (Lazarev et al., 2020). The lower Maeotian first comprises offshore deposits, followed by alternating offshore, shoreface and back barrier-lagoon environments. The presence of freshwater mollusks in shallow water facies, and oligohaline microfauna in deeper water facies, suggests that the deeper basin remained brackish, whereas marginal environments had a freshwater influence. In the upper Maeotian, progradation of deltaic environments with delta-front parasequences and abundant freshwater fauna reveal a relative base-level lowering occurring between 6.5 and 6.3 Ma. Abrupt replacement of deltaic deposits by deeper water offshore facies subsequently announces a late Maeotian transgression starting at 6.3 Ma (Lazarev et al., 2020). The Maeotian-Pontian transition is marked by the occurrence of a rich foraminifera assemblage including *Ammonia*, *Ammotium*, *Quinqueloculina*, *Prosononion* and *Streptochilu*s genera. Shortly after, the first indicative Pontian mollusk *Eupatorina littoralis littoralis* represents a first immigration pulse originating from Aegean region (Figure 6; Lazarev et al., 2020). A subsequent immigration pulse is marked by new mollusk taxa of Pannonian origin (*Pseudoprosodacna* sp., *Didacna* sp., *Congeria rhomboidea* and *Paradacna abichi*, *Valenciennius* spp.) (Figure 6). During the Odessian (lower Pontian), distal littoral environments persisted and salinity returned to brackish values of ~8 (Stoica et al., 2013). The Portaferrian (middle Pontian) was marked by a strong regression and water levels dropped (ca. 100 m) giving rise to freshwater fluvial environments with channels and floodplains (Jipa et al., 2009; Stoica et al., 2013). Another transgression marks the base of the Bosphorian (upper Pontian) when a noticeable change to more distal facies and a return to anomalohaline water (7–8 salinity) is observed. During the Dacian stage, the basin progressively filled (Jipa et al., 2009) and deltaic sediments became prominent (Jorissen et al., 2020). The top of the Dacian stage marks the end of brackish delta-front deposition and is overlain by fluvial and fresh-water lacustrine Romanian stage (Van Baak, Mandic, et al., 2015). A short return of brackish fauna and deeper environments is observed at the so-called "Plescoi flooding event (Pană et al., 1968; Van Baak, Mandic, et al., 2015). Upwards, the section is dominated by fluvial and fresh-water lacustrine conditions, marking the progressive continentalization of the Dacian Basin.

We used ostracods from the Slanicul de Buzau section and added 39 new $^{87}Sr/^{86}Sr$ data points to the earlier acquired results from Rîmnicu Sărat (Vasiliev et al., 2010), extending and refining in this way the Dacian Basin $^{87}Sr/^{86}Sr$ record from the late Miocene (Khersonian) to the Pleistocene (Romanian Stage). Age constraints for Slanicul de Buzau section are provided by biostratigraphy coupled to magnetostratigraphy (Grothe et al., 2018; Lazarev et al., 2020; Van Baak, Mandic, et al., 2015). Additionally, the section is correlated by magneto-biostratigraphy to the previously investigated Rîmnicu Sărat section, 15 km to the north (Stoica et al., 2013; Vasiliev et al., 2004, 2010).

4. Methods

We measured the $^{87}Sr/^{86}Sr$ only on ostracods (Figure 3). The choice for ostracods is twofold, (a) they occur abundantly in the fresh to brackish deposits of the Paratethys, while these environments are generally not suitable for the occurrence of foraminifera and other typical marine organisms; (b) ostracods bear in general low ornamentation and they molt their entire shell in one event. Consequently, these shells are relatively easy to clean because, in contrast to foraminifera, they do not consist of separate chambers potentially filled with other material contaminating the isotopic signal.

All $^{87}Sr/^{86}Sr$ analyses were performed on handpicked ostracods that were separated from the bulk sediment by disaggregation in sodium carbonate solution and wet sieving to retain the >125 μm fraction. The ostracod samples were not crushed during the cleaning procedure. Clays were removed by washing five times in MilliQ®, five times in methanol (96%) and by ~5–30 s cleaning in an ultrasonic bath. The washing procedure was then repeated three times. As the last cleaning step, the ostracod samples were rinsed five times with MilliQ® and dried overnight in a clean hood.

4.1. Diagenetic Evaluation

Selected cleaned samples were evaluated for potential diagenetic alteration using trace element analysis and scanning electron microscopy (SEM). The selected samples from Slanicul de Buzau were ablated using a Lambda Physik Excimer 193 nm laser with GeoLas 200Q optics coupled to Micromass Platform quadrupole

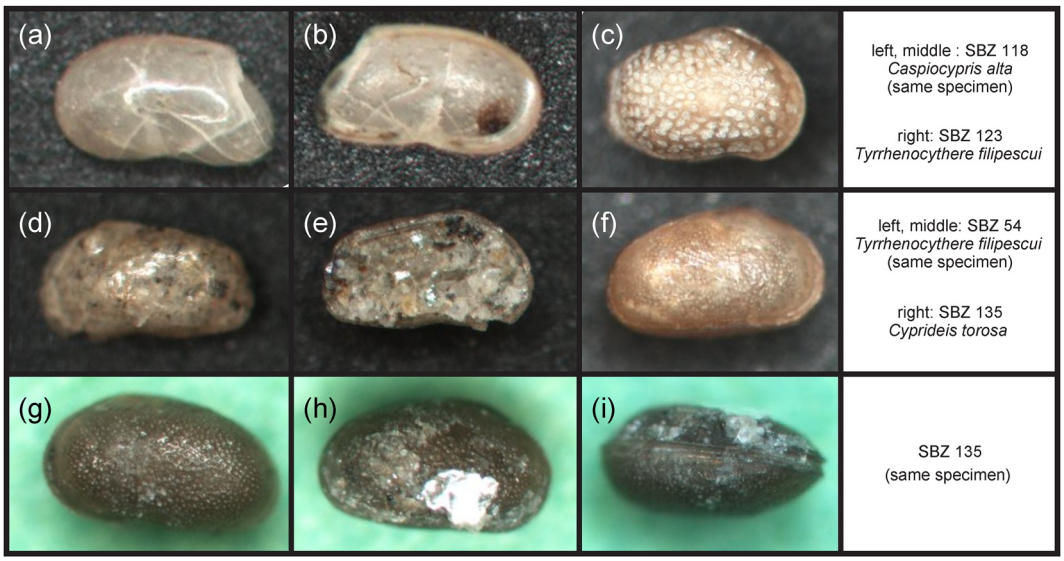
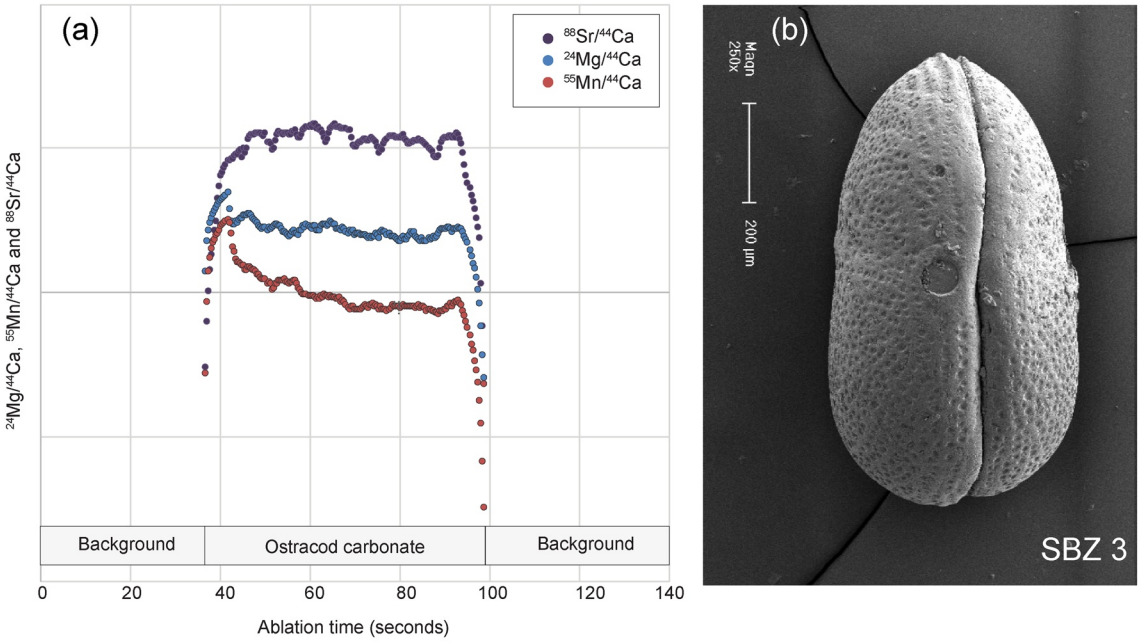


Figure 3. Photographs of the five representative ostracod specimens before cleaning for analysis. Sample SBZ 118 represents a clean and pristine ostracod shell (panels a and b), while the ornaments of specimen SBZ 123 are filled with small whitish crystals (panel c). Specimen SBZ 54 is completely filled with large quartz and/or mica clasts cemented from the sediment (panel d and e). Carapaces of sample SBZ 135 seem clean from the outside (panel f and g), but also contain specimens with visible crystals on the outside (panel h and i).

ICP–MS at Utrecht University. Ablation was performed in a mixed atmosphere of helium and argon with a repetition rate of 6 Hz and spot diameter of 80 μm. Instrument calibration was performed against U.S. National Institute of Standards and Technology SRM 610 glass using the concentration data of Jochum et al. (2011) with ^{44}Ca as an internal standard. Monitored masses included ^{24}Mg, ^{26}Mg, ^{27}Al, ^{43}Ca, ^{44}Ca, ^{55}Mn, ^{88}Sr, ^{138}Ba and ^{238}U. The reported values are normalized against ^{44}Ca to overcome the varying response (counts per second) during ablation that generates variable quantity of removed material. To reduce spectral interferences of the minor Ca isotopes (^{42}Ca, ^{43}Ca, ^{44}Ca), a collision and reduction cell was used (Mason & Kraan, 2002).

4.2. Strontium Isotope Analyses

To determine ^{87}Sr/^{86}Sr, 0.01–0.6 mg of ostracod(s) valves, separated, extracted and cleaned from 54 levels were dissolved in 0.5 ml acetic acid and centrifuged to separate the solution from any residues. The separation of the individual ostracods into singular valves was performed to avoid dissolving putative residue and to ensure appropriate sample weight as some of the specimens were larger than 0.6 mg. Despite the thorough cleaning using an ultrasonic bath, three out of the total of 39 samples yielded visible residues of non-dissolved parts. These samples are indicated with an asterisk in Table 1. The solution was then pipetted into a separate beaker and evaporated to dryness and the non-dissolved part of the sample was discarded. The residue after drying the solution was re-dissolved in concentrated HNO_3 (1 drop), evaporated to dryness and again dissolved in conc. HNO_3 (2 drops) and evaporated to dryness. The samples were then dissolved in 0.5 ml 3N HNO_3 and stored on a hotplate for 1 h. Samples were put in an ultrasonic bath for 15 min before chromatographic separation. 0.4 ml of the samples was introduced to chromatographic columns composed of "Eichrom Sr spec" ion exchange resin to isolate the strontium fraction. This fraction was dried and nitrated twice with two and one drop(s) of concentrated HNO_3, respectively. Strontium isotope analyses were carried out on a Finningan MAT 262 thermal ionization mass spectrometer at the VU University (Amsterdam) running in the 'static' mode. Strontium isotope ratios were corrected for instrumental mass fractionation by normalizing to ^{86}Sr/^{88}Sr = 0.1194. Samples were analyzed over a two-year period during which degradation of Faraday cup performance led to replacement of some of the Faraday cups and changes in the cup configurations used. Data are reported for three distinct analytical periods. Repeated measurements of the international standard NBS-987 yielded averages of respectively 0.710273 ± 0.000008 (2σ), n = 28;



(c)

Concentration						Error				
isotope used	Element	SBZ3	SB5	SB20	SBZ162	Element	SBZ3	SB5	SB20	SBZ162
Mg24	Mg	3165	2067	6678	2070	Mg	191	129	408	125
Mg26	Mg	3231	2084	6474	2031	Mg	345	233	701	219
Al27	Al	520	<40	2461	<36	Al	34	15	136	14
Ca43	Ca	400233	400233	400233	400233	Ca	13539	13141	13541	13085
Ca44	Ca	405134	414854	413108	407809	Ca	16963	17569	17456	16951
Mn55	Mn	571	3069	5519	1450	Mn	37	208	364	94
Sr88	Sr	5594	3028	1329	1086	Sr	264	147	64	51
Ba138	Ba	1050	1148	536	367	Ba	61	70	32	22
U238	U	0	3	5	2	U	0	0	1	0

Figure 4. (a) Time resolved laser-ablation inductively coupled plasma mass spectrometry (LA ICP–MS) data plotted on a linear scale for a representative cleaned sample from the Dacian Basin. (b) The ablation crater is observed in the scanning electron micrograph (SEM) of ostracods specimen *Cyprideis* sp. (SBZ 3) from the Slanicul de Buzau (see methods section for the procedure). Values (also listed in the table from panel c) are normalized against ^{44}Ca to correct for variations in ablation rates (counts per second). A moving average is used to filter out interference between laser pulse frequency and cycle time of the mass spectrometer. Some remaining high frequency variability is still visible as an artifact. Counting rate peaks at the start of the analysis indicates that the outside of the shell included some clay minerals and/or coating that were not removed despite the cleaning procedure, for example, Al/Ca and/or Mn/Ca. Once the laser beam samples the shell itself, however, the Sr/Ca remains stable, which indicates that there was no appreciable alteration of the strontium in the shell after deposition. (c) Elemental concentrations and errors were calculated for the inner part of the shell.

0.710259 ± 0.000011 (2σ), n = 18; 0.710257 ± 0.000006 (2σ), n = 22. Data were normalized to the long term average value obtained for NBS 987 over the previous 5 years of 0.710254 ± 0.000005 (2SE), n > 100. The strontium blanks determined were <330 pg (avg. 197) and negligible relative to the overall amount of strontium analyzed from the ostracods (>100 ng).

5. Diagenetic Evaluation: Reliability of the Strontium Isotope Ratios

The ablation profiles show that, despite the cleaning procedure, there are still some "coatings" remaining on the outside of the ostracod shells (Figure 4). These coatings, indicated by Mn peaks, are only present at the outer parts. Similar peaks are also visible in the ablation profiles from samples of Rîmnicu Sărat (Vasiliev et al., 2010), while the ablation profiles for the Black and Caspian Seas lack these pronounced peaks (Grothe et al., 2020). The exact nature of the Mn-Al-rich crusts is unknown but seems typical for the Dacian Basin. Despite the presence of these coatings we consider the measured $^{87}Sr/^{86}Sr$ reliable, because, for all analyzed ostracod valves, the LA-ICPMS ablation tracks showed constant Sr/Ca ratio through the same profiles indicating that post-depositional processes did not affect the strontium content of the shells. Elemental concentrations were calculated for the inner part of the shell (gray zone in Figure 4). Some samples are characterized by a relatively high Mn concentration, but there appears to be no higher Sr concentrations

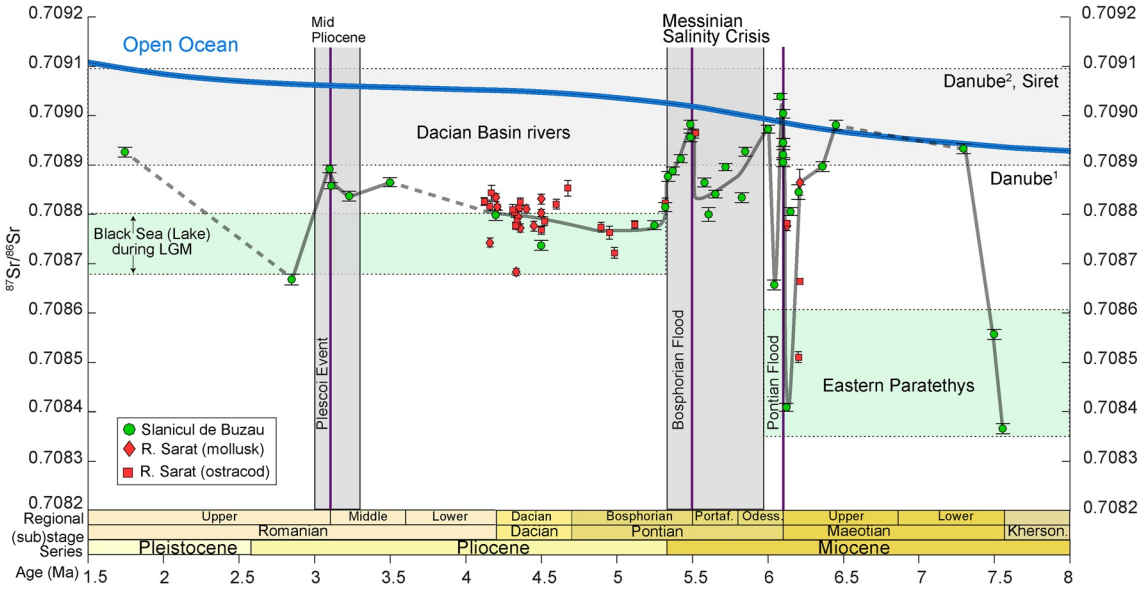


Figure 5. Late Miocene-Pliocene $^{87}Sr/^{86}Sr$ records of the Dacian Basin. Green circles show $^{87}Sr/^{86}Sr$ measured on ostracods from the Slanicul de Buzau section, while red squares and diamonds depict $^{87}Sr/^{86}Sr$ of ostracods and *mollusks* from Rîmnicu Sărat (Vasiliev et al., 2010), respectively. The gray line represents an interpretation of the average $^{87}Sr/^{86}Sr$ curve in the Dacian Basin. Vertical purple lines indicate "flooding" events in the Dacian Basin based on faunal studies (e.g., Stoica et al., 2013; Van Baak, Mandic, et al., 2015; Lazarev et al., 2020). The quasi-horizontal blue trend-line represents the $^{87}Sr/^{86}Sr$ of the open ocean through time (McArthur et al., 2012). Dashed lines indicate the $^{87}Sr/^{86}Sr$ of the main rivers draining in the Dacian and the Black Sea Basins, the horizontal bar indicates the range of $^{87}Sr/^{86}Sr$ in the Black Sea during the Last Glacial Maximum.

in these shells. In contrast, Ba concentrations show roughly a negative correlation with Sr concentrations. High Ba concentrations are typical for freshwater-settings as Ba concentrations are relatively high in river water (Figure 4). The observed trend in Ba-Sr concentrations are explicable, because SBZ-3 is probably deposited in a freshwater lake, while faunal assemblages suggest more brackish conditions for SBZ-162 (Figure 4). Some of the studied ostracods from Slanicul de Buzau yield crystals on the ornaments or inside their shell (Figure 4). Despite the mechanical cleaning procedure, we were unable to remove all these crystals. Specimens with large visible crystals were therefore excluded. However, specimens with small crystals in the ornaments were processed. To avoid any potential alteration of the original $^{87}Sr/^{86}Sr$, we dissolved all our samples in acetic acid instead of the more commonly used nitric acid. This weak acid dissolves carbonates before affecting more resistant minerals. By pipetting off the dissolved strontium (<15 min), potential contamination from a more acid-resistant strontium source is minimized. We are therefore confident that the measured strontium isotope ratios mainly represent the carbonate and therefore the water it was precipitated from.

6. Strontium Isotope Ratios of the Dacian Basin

Our $^{87}Sr/^{86}Sr$ of ostracod valves from the Slanicul de Buzau section range from 0.70835 to 0.70905 (Table 1; Figure 5). These ratios are in good agreement with the strontium isotope record from the Rîmnicu Sărat section (Figure 5; Vasiliev et al., 2010), illustrating that these ratios represent a regional signal and that both datasets can be linked, together forming a 5 Myr record of Dacian Basin connectivity.

The lowest isotopic ratios (0.70835) are recorded at the base of the Maeotian (7.6 Ma), followed by a rapid increase to open ocean and local river ratios (0.7089–0.7090). While there subsequently is a gap in the record, values at 6.4 Ma are similarly high (Figure 5). In the upper Maeotian (6.2 Ma) the isotopic ratios drop to values between 0.70880–0.070885, after which they rise again. At ca. 6.1 Ma, this trend is accentuated by a sudden and distinctive lowering in $^{87}Sr/^{86}Sr$ to 0.7084, directly followed by a well-defined rise with ratios reaching the open ocean and local river values. The subsequent data point suggests a return to ~0.70865. $^{87}Sr/^{86}Sr$ then rise to values ranging between 0.7088–0.7089, followed by a gradual decrease during the 6.0–5.6 Ma interval (Figure 5). At 5.5 Ma, ratios peak again, after which the $^{87}Sr/^{86}Sr$ show a consistent lowering

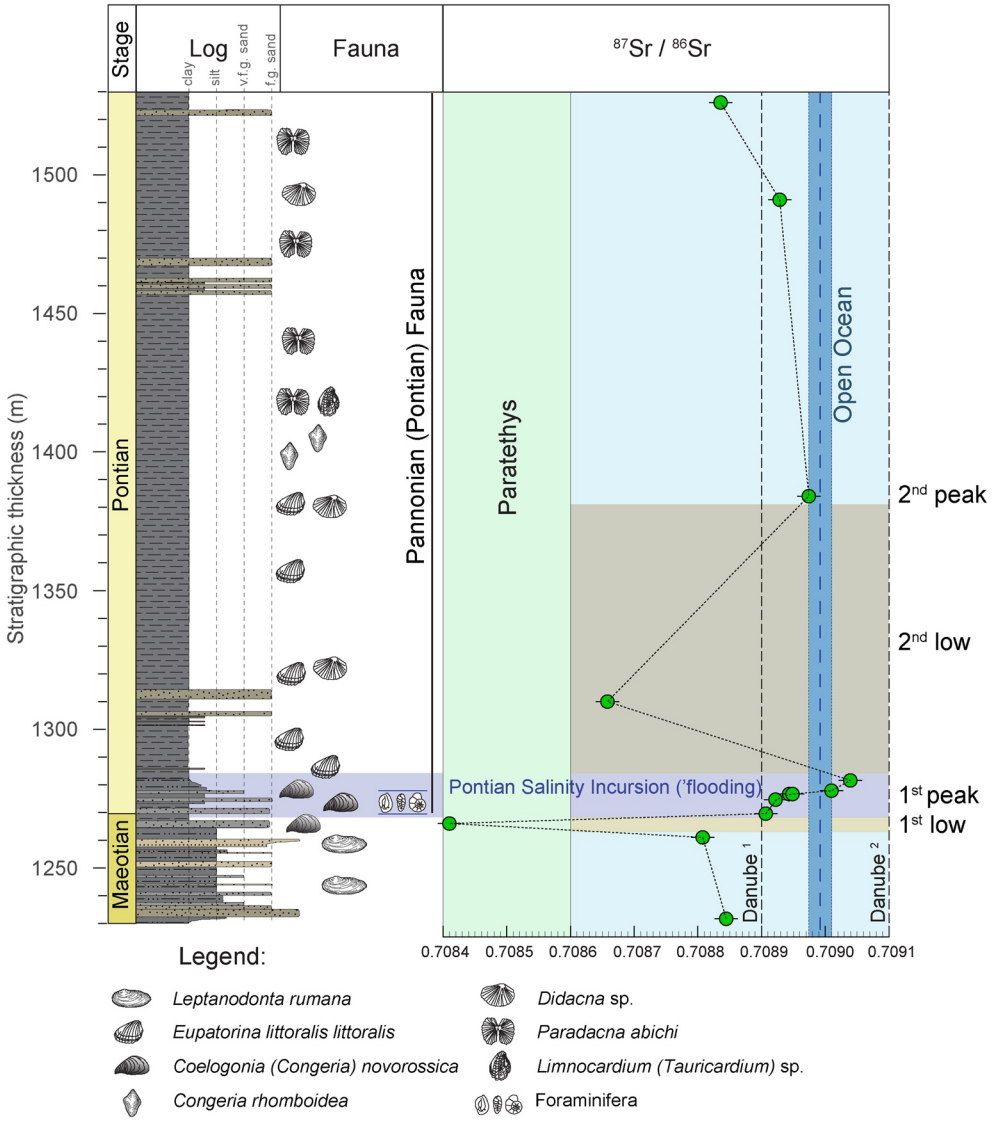


Figure 6. Lithology, fauna and $^{87}Sr/^{86}Sr$ of the interval straddling the Maeotian-Pontian Boundary at Slanicul de Buzau, based on a recently updated age model (Lazarev et al., 2020). The thick blue line resembles the average $^{87}Sr/^{86}Sr$ of the open ocean between 6.25–5.8 Myr ago (McArthur et al., 2012). Vertical dashed lines indicate the $^{87}Sr/^{86}Sr$ of the Danube River according to: Palmer & Edmond (1992) and Zitek et al. (2015).

to 0.7088 (Figure 8a). Between 5.3–4 Ma, $^{87}Sr/^{86}Sr$, predominantly determined previously at Rîmnicu Sărat, vary between 0.7087–0.70885 and do not show major shifts (Vasiliev et al., 2010). The $^{87}Sr/^{86}Sr$ for the Romanian Stage are based on six data points (Figure 5). Around 3.2 Ma, there is a rise in the $^{87}Sr/^{86}Sr$ from roughly 0.70885 to 0.70890, and then a significant drop to 0.7087. The single data point within the late Romanian is close to the Danube's $^{87}Sr/^{86}Sr$ of 0.7089 (Palmer & Edmond, 1992) (Figure 5).

7. Discussion: Origin of the $^{87}Sr/^{86}Sr$ Signal

Considering the late Miocene paleogeographic setting of the Dacian Basin, the most likely source of low $^{87}Sr/^{86}Sr$ is the Eastern Paratethys (unified Black Sea-Caspian Sea), which was characterized by $^{87}Sr/^{86}Sr$ of ca. 0.70825 before the Pontian Flood (Figures 7 and 8; Grothe et al., 2020). The high $^{87}Sr/^{86}Sr$ could have originated from three different sources. The first is an inflow of Lake Pannon waters, derived from the upstream part of the present-day Danube catchment. A second source that could have provided the high

Table 1
$^{87}Sr/^{86}Sr$ From Slanicul de Buzau Record

Sample name	(Sub) stage	Age (Ma)	$^{87}Sr/^{86}Sr$	2σ	Species
8d/2016	Lowermost Maeotian	7.63	0.708353	0.000015	*Cyprideis sp. & Ammonia*
8J/2016	Lower Maeotian	7.60	0.708587	0.000015	*Cyprideis sp. & Ammonia*
SRM 16/AL 08	Lower Maeotian	7.34	0.708938	0.000015	*Cyprideis sp.*
SRM 16/AL 15	Upper Maeotian	6.46	0.708981	0.000015	*Cyprideis sp.*
SRM 16/AL 19	Upper Maeotian	6.43	0.708903	0.000015	*Cyprideis sp.*
SRM 16/SL 11	Upper Maeotian	6.17	0.708492	0.000015	*Cyprideis sp.*
SBZ 3	Upper Maeotian	6.14	0.708845	0.000015	*Cyprideis sp.*
SBZ 8	Upper Maeotian	6.11	0.708806	8E-06	*Cyprideis sp.*
SBZ 10	Upper Maeotian	6.11	0.708409	8E-06	*Cyprideis sp.*
SBZ 14	Lower Pontian (Odessian)	6.10	0.709039	0.000006	*Pontoniella & Cyprideis sp*
SB 5	Lower Pontian (Odessian)	6.10	0.708906	0.000009	*Cyprideis sp.*
SB 42	Lower Pontian (Odessian)	6.10	0.709004	0.000009	*Cyprideis sp.*
SB 25	Lower Pontian (Odessian)	6.10	0.708946	8E-06	*Cyprideis sp.*
SB 25	Lower Pontian (Odessian)	6.10	0.708945	8E-06	*Cyprideis sp., Leptocythere sulakensis*
SB 20	Lower Pontian (Odessian)	6.10	0.708921	0.000010	*Cyprideis sp.*
SB 20	Lower Pontian (Odessian)	6.10	0.708787	0.000015	*Cyprideis sp.*
SBZ 17	Lower Pontian (Odessian)	6.07	0.708657	0.000010	*Cyprideis sp.*
SBZ 22	Lower Pontian (Odessian)	6.00	0.708973	8E-06	*Caspiocypris*
SBZ 32	Lower Pontian (Odessian)	5.85	0.708927	0.000009	*Camptocypria fragment*
SBZ 35	Lower Pontian (Odessian)	5.83	0.708834	0.000010	*Pontoniella lotzi*
SBZ 54*	Middle Pontian (Portaferrian)	5.72	0.708896	0.000007	*Tyrrhenocythere filipescui*
SBZ 64	Middle Pontian (Portaferrian)	5.65	0.708841	8E-06	*Cyprideis torosa*
SBZ 69	Middle Pontian (Portaferrian)	5.61	0.708800	0.000014	*Candona sp.*
SBZ 74	Middle Pontian (Portaferrian)	5.58	0.708865	0.000009	*Tyrrhenocythere filipescui & Amplocypris sp.*
SBZ 84	Upper Pontian (Bosphorian)	5.49	0.708982	0.000009	*Tyrrhenocythere filipescui*
SB 162	Upper Pontian (Bosphorian)	5.49	0.708956	0.000009	*Tyrrhenocytheresp.*
SBZ 100	Upper Pontian (Bosphorian)	5.42	0.708913	0.000008	*Tyrrhenocythere filipescui & Caspiolla ossoinanensis*
SBZ 111*	Upper Pontian (Bosphorian)	5.37	0.708888	8E-06	*Tyrrhenocythere filipescui*
SBZ 118	Upper Pontian (Bosphorian)	5.34	0.708877	0.000010	*Tyrrhenocythere filipescui*
SBZ 123	Upper Pontian (Bosphorian)	5.32	0.708815	0.000009	*Caspiocypris alta (fragments)*
SBZ 135*	Upper Pontian (Bosphorian)	5.25	0.708778	0.000009	*Cyprideis torosa*
SBD 30	Lower Dacian	4.50	0.708737	0.000010	*Cyprideis sp.*
SBD 17	Upper Dacian	4.20	0.708798	0.000010	*Cyprideis sp.*
ER 8	Middle Romanian	3.50	0.708865	0.000009	*Cyprideis sp.*
ER 30	Middle Romanian	3.23	0.708837	0.000010	*Cyprideis sp.*
BR 3	Middle /Upper Romanian	3.11	0.708858	0.000006	*Cyprideis sp.*
BR 2b	Middle /Upper Romanian	3.10	0.708892	8E-06	*Cyprideis sp.*
ER 44	Upper Romanian	2.85	0.708668	1.1E-05	*Ilyocypris bradyi*
ER 96	Upper Romanian	1.75	0.708926	0.000010	*Ilyocypris bradyi*

Note. The samples with asterisk yielded visible residues.

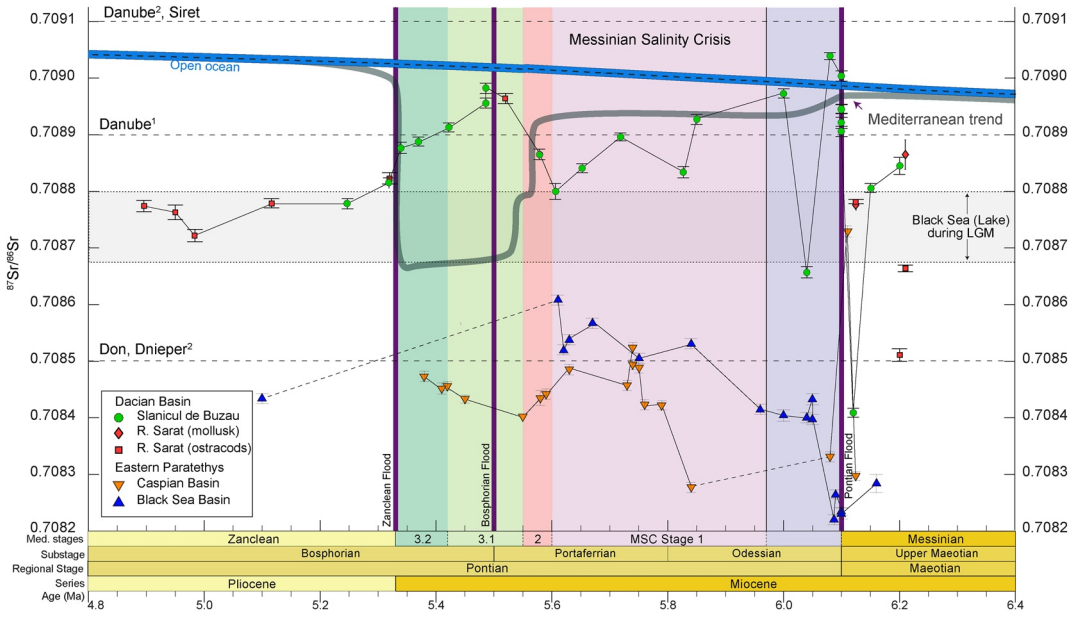


Figure 7. Comparison of $^{87}Sr/^{86}Sr$ records from Slanicul de Buzau (Dacian Basin) with the Black Sea, Caspian and Mediterranean Basins. Green circles show $^{87}Sr/^{86}Sr$ measured on ostracods from the Slanicul de Buzau section; red squares and diamonds depict $^{87}Sr/^{86}Sr$ of ostracods and mollusks from Rîmnicu Sărat, respectively (Vasiliev et al., 2010). Blue and orange triangles represent $^{87}Sr/^{86}Sr$ from Zheleznyi Rog (Black Sea) and Adzhiveli (Caspian), respectively (Grothe et al., 2020). The gray line represents an interpretation of the average $^{87}Sr/^{86}Sr$ in the Mediterranean Basin (after Grothe et al., 2020 from various sources see Roveri, Flecker, et al. (2014) for an overview, Schildgen et al. (2014) and Reghizzi et al. (2017; 2018)). Error bars represent analytical errors (2σ). The quasi-horizontal blue trend-line represents the $^{87}Sr/^{86}Sr$ of the open ocean through time (McArthur et al., 2012). Vertical purple lines indicate "flooding" events in the Dacian and Mediterranean Basin based on faunal studies (e.g., Stoica et al., 2013; Roveri, Flecker, et al., 2014). Dashed horizontal lines indicate the $^{87}Sr/^{86}Sr$ of the main rivers in the Dacian Basin and the Black Sea Basin, the horizontal bar indicates the range of $^{87}Sr/^{86}Sr$ in the Black Sea during the Last Glacial Maximum (LGM). The terminology for the different stages of the Messinian Salinity Crisis (MSC) follows Roveri, Flecker, et al. (2014): 1. Primary Lower Gypsum, 2. the MSC acme, 3. Upper Evaporites and Lago Mare.

$^{87}Sr/^{86}Sr$ is the late Miocene Balta delta that was sourced from the external West and East Carpathians in analogy with for example, the present-day Siret River (Figure 1). Finally, this signal could have a marine origin, and signify that water entered the basin through the Mediterranean and Black Sea. All three sources are characterized by $^{87}Sr/^{86}Sr$ values between 0.7089-0.7091 (Palmer & Edmond, 1992; Roveri, Lugli, et al., 2014; Zitek et al., 2015).

7.1. The Early Maeotian Transgression

The early Maeotian transgression, at ~7.6 Ma, starts with the lowest $^{87}Sr/^{86}Sr$ (0.70835), which likely originated from the neighboring Black Sea Basin, related most probably to an increasingly unified Eastern Paratethys water level. A transgression similar to the one at 7.6 Ma would have required the elevation of the water level in the unified Eastern Paratethys. In this way Eastern Paratethys could have been able to spill into the Dacian Basin. If the transgression was expressed by rising shorelines of the Dacian Lake, this could only happen if the combined Black and Caspian lakes had been previously endorheic (as suggested by Palcu et al., 2019) and then topped up with saltier water from the Mediterranean. Alternatively the unified Eastern Paratethys and Dacian Basin lakes were already connected both ways and Maeotian transgression, at ~7.6 Ma is expressed by new, saltier water source originating from the Mediterranean leading a pronounced shift in $^{87}Sr/^{86}Sr$ of the unified Eastern Paratethys and Dacian basin.

During the early Maeotian, $^{87}Sr/^{86}Sr$ rise to a maximum of 0.70893, documented at 7.3 Ma. The corresponding interval is characterized by barrier island and back-barrier lagoon deposits (Lazarev et al., 2020). The Slanicul de Buzau section was at that time located at the shoreline, at short distance away from the mouth

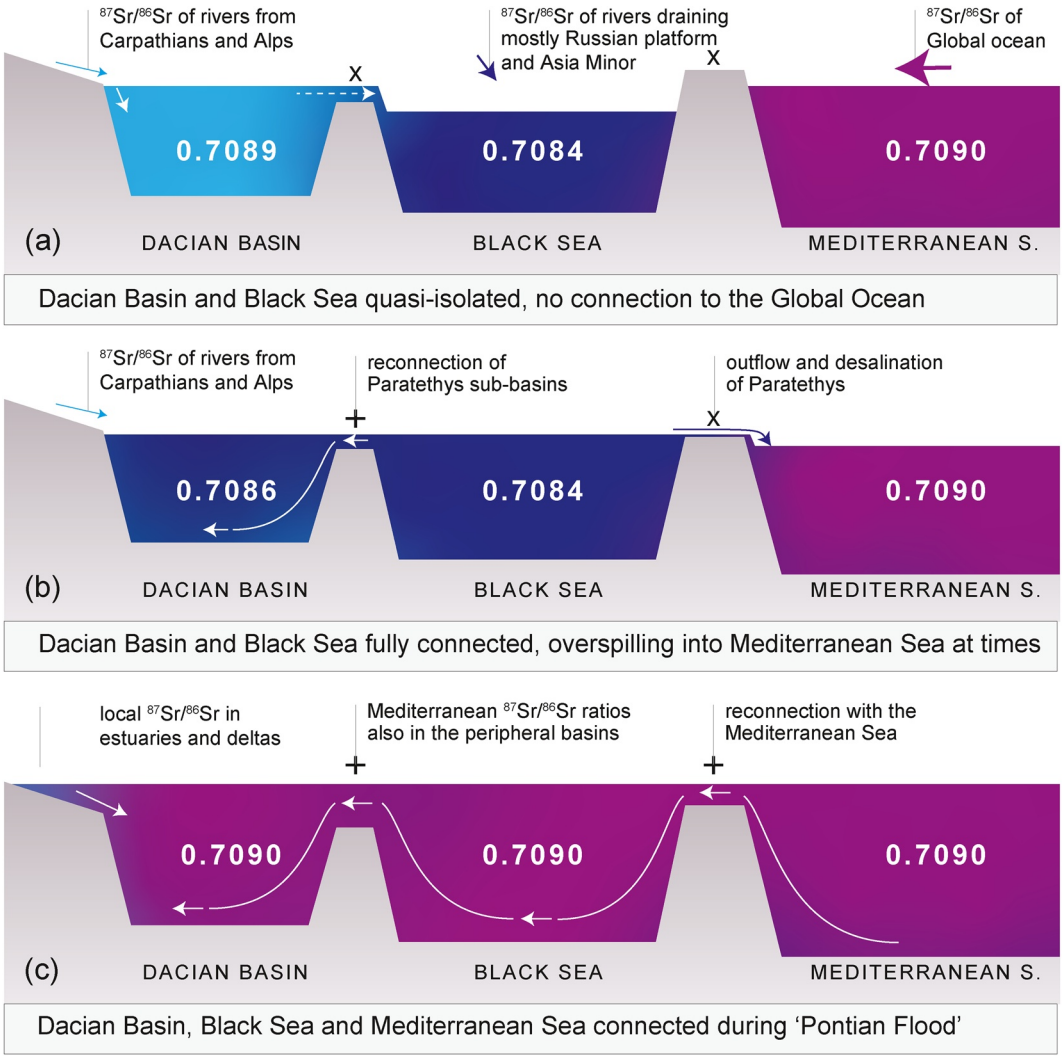


Figure 8. Schematic cross-section showing the changes in connectivity of the Dacian Basin with the Black Sea and Mediterranean. The $^{87}Sr/^{86}Sr$ at different times for different basins are displayed in white. (a) Dacian Basin and Black Sea were quasi-isolated and not connected to the global ocean via the Mediterranean. The Dacian Basin had an outflow to the Black Sea at times with positive water budget; (b) Dacian Basin and Black Sea were fully connected and overspilling into the Mediterranean at times. Dacian Basin and Black Sea had at times an outflow to the Mediterranean; (c) Dacian Basin, Black Sea and Mediterranean were connected during the "Pontian flooding", at 6.1 Ma.

of the Balta delta to the north (analogous to the present-day Dniester, Prut, southern Bug and Siret rivers; De Leeuw et al., 2020; Matoshko et al., 2016). We thus attribute the increase in $^{87}Sr/^{86}Sr$ ratios to an increased influence of water coming from the Balta delta. The predominance of brackish-water ostracods in offshore deposits precludes a strong marine influence, while a Danubian influence seems unlikely given that the Maeotian fauna is distinct from that of Lake Pannon at this time. We therefore attribute the increase in $^{87}Sr/^{86}Sr$ to an increased proportion of local rivers (i.e., Balta delta). At 6.5 Ma, the $^{87}Sr/^{86}Sr$ is similarly high, between 0.7089–0.7091. Given that this interval is characterized by deposition on the Balta delta-front (Lazarev et al., 2020), we also attribute this elevated value to water supplied by this delta. An abrupt replacement of deltaic deposits by relatively deep water offshore facies provides evidence for a major transgression that started in the late Maeotian, at 6.3 Ma. Offshore environments, only rarely interrupted by delta front sedimentation, persist from this time into the early Pontian. Several pulses with brackish water microfauna with *Typhlocyprella* sp. occur in the 6.3–6.1 Ma interval and suggest a periodic outflow of Lake Pannon into the Dacian Basin (Lazarev et al., 2020). In the 6.3–6.1 Ma interval, that is, from the late Maeotian initiation of distal environments to the Pontian salinity incursion, the strontium ratios are progressively lowering.

We interpret this as a gradually increasing contribution of Eastern Paratethys waters to the Dacian Basin, which apparently outcompeted the high $^{87}Sr/^{86}Sr$ from local rivers and the Pannonian Basin. It thus seems that higher water levels led to the establishment of a restricted connection between the Dacian Basin and the Black Sea that allowed gradual mixing.

7.2. The Pontian Flood

The Pontian Flood at ~6.1 Ma, recently renamed the "Pontian Salinity Incursion" (Lazarev et al., 2020), is marked by large and rapid shifts in $^{87}Sr/^{86}Sr$ (Figures 5–7). Such rapid $^{87}Sr/^{86}Sr$ changes are observed in both the Rîmnicu Sărat and Slanicul de Buzau sections.

Detailed integration of the lithological and faunal evolution to the $^{87}Sr/^{86}Sr$ variations from the Maeotian-Pontian transition interval at Slanicul de Buzau provides the following observations. Within the uppermost Maeotian, a remarkable interval between 1,230 – 1,267 m exhibits numerous current-ripple cross-laminated sandstones with freshwater mollusks *Leptanodonta rumana* (Figure 6). This interval has been recently interpreted as a mouth bar-delta front (Lazarev et al., 2020). $^{87}Sr/^{86}Sr$ are between 0.70880–0.70885, somewhat lower than the ratios for water from the present-day Danube (Palmer & Edmond, 1992) and Siret rivers (Zitek et al., 2015), suggesting some admixture of Eastern Paratethys water.

An appreciably lower $^{87}Sr/^{86}Sr$ of 0.7084 is found at the very end of the deltaic interval (1,266 m), which is similar to $^{87}Sr/^{86}Sr$ of the Black Sea during the lower Pontian (Figure 6). This indicates that the Dacian Basin at this time had nearly completely come under the influence of the Black Sea Basin, experiencing a more functional water exchange.

This first low ratio is followed by a sharp and consistent rise in $^{87}Sr/^{86}Sr$ from 0.70890 to 0.70905 in the interval of the Pontian salinity incursion (Figure 6, between 1,269.8 m and 1,281.5 m). This interval is characterized by shell accumulations of *Congeria (Andrusoviconca) amygadaloides novorossica*, benthic calcareous foraminifera and the planktonic foraminifer *Streptochilus* spp. (Stoica et al., 2013; Figure 6). The presence of marine fauna suggests that the $^{87}Sr/^{86}Sr$ maximum is very likely related to marine influxes (McArthur et al., 2012; Palmer & Edmond, 1992; Roveri, Lugli, et al., 2014; Zitek et al., 2015). Remarkably, marine $^{87}Sr/^{86}Sr$ values have not been recorded at the Pontian Flood in the Taman section of the Black Sea Basin (Grothe et al., 2020). Potential explanations could be that bottom water anoxia prevented the presence of ostracods during peak-flooding (Grothe et al., 2020), or maybe because the exact interval was missed in Taman, where the corresponding interval is much thinner due to the much lower sedimentation rates than at Slanicul de Buzau. The rapid and large changes in $^{87}Sr/^{86}Sr$ at Slanicul de Buzau across the Pontian flooding interval emphasize the importance of high-resolution sampling.

After a $^{87}Sr/^{86}Sr$ maximum is reached (Figure 6, 1,286 m), the first indicative Pontian mollusk *Eupatorina littoralis littoralis*, a migrant from the Aegean area, are found, marking the traditional base of the Pontian stage (Figure 6). The $^{87}Sr/^{86}Sr$ value in the interval with Pannonian fauna (Figure 6, 1,269.8 m) has an appreciably lower isotopic ratio (0.70865). This indicates that $^{87}Sr/^{86}Sr$ values were again briefly dominated by the Black Sea where the marine influence had apparently disappeared. Alternatively, the observed trends at Slanicul de Buzau can also be explained by varying the amounts of Lake Pannon and Black Sea waters in the Dacian Basin.

A second period of low $^{87}Sr/^{86}Sr$ and the introduction of Pannonian mollusks (Figure 6; *Didacna* spp., *Congeria rhomboidea* and *Paradacna abichi*, *Valenciennius* spp) is followed by monotonous marls, representing the deepest facies in the studied record (Figure 6). In this interval, $^{87}Sr/^{86}Sr$ are higher, typically around 0.7088. The absence of marine fauna and the dominance of Pannonian derived ostracods, mollusks and dinoflagellates in this interval (Grothe et al., 2018) suggest that the elevated $^{87}Sr/^{86}Sr$ are most likely related to the increased contribution of Lake Pannon outflow and local river waters in the Dacian Basin (Figure 8a). The water inflow from Lake Pannon would have brought water source with, Danube like $^{87}Sr/^{86}Sr$ into the Dacian Basin modifying the marine like isotopic signature. The direction of the water flow is this case would be one way. However, the fauna, including ostracods, could migrate against the direction of the water flow. The water flow direction is important for the $^{87}Sr/^{86}Sr$ isotopes but, if the salinity of the inflow basin (i.e., Lake Pannon) would have been the same as the salinity of the outflow (i.e., Dacian Basin), than the fauna could have easily migrated both ways.

These observations highlight that the Paratethyan gateways separating the basins were limited in size, so that minor variations in sea level or run-off caused appreciable differences of in- and outflowing water.

7.3. The Dacian Basin in MSC Times

During the first stage of the MSC (Primary Lower Gypsum), $^{87}Sr/^{86}Sr$ in the Dacian Basin gradually decrease while the $^{87}Sr/^{86}Sr$ in the Black Sea and Caspian Basin increase (Figures 7 and 8). These converging curves indicate that progressive mixing of the Dacian Basin and Eastern Paratethys occurred in the time interval 5.9–5.6 Ma. At the beginning of MSC Stage 2, the Dacian and Caspian curves suddenly start to diverge again, indicating progressive restriction. This interval corresponds to the peak MSC (halite deposition occurring between 5.60 to 5.55 Ma) where the Paratethys water level dropped in concert with the Mediterranean that experienced its major lowstand. Lowering the base level will lead to restricted connectivity, which explains why the $^{87}Sr/^{86}Sr$ curve of the Dacian Basin evolves to the high, local river values while the $^{87}Sr/^{86}Sr$ of the Caspian Basin became dominated by the low ratios of the Volga river (Figure 7).

Another period of elevated $^{87}Sr/^{86}Sr$ is observed in the Dacian Basin during the so-called "Bosphorian Flood", magnetostratigraphically dated at 5.5 Ma in Rîmnicu Sărat Valley, assuming a constant sedimentation rate (Figure 7; Vasiliev et al., 2004). A similar rise in $^{87}Sr/^{86}Sr$ has not been observed in the strontium isotope records of the Black Sea where an assumed hiatus between ca. 5.6 and 5.3 Ma marks the sedimentary succession in the Zheleznyi Rog section (Krijgsman et al., 2010; Vasiliev et al., 2011). In the adjacent Caspian Basin, no samples have been analyzed at ~5.5 Ma (Grothe et al., 2020). For the Bosphorian Flood, the two potential sources of high $^{87}Sr/^{86}Sr$ are marine waters from the Mediterranean and/or increased outflow waters of Lake Pannon. The Bosphorian Flood roughly corresponds to the base of MSC Stage 3 (Roveri, Flecker, et al., 2014), when the Mediterranean Basin is characterized by relatively low $^{87}Sr/^{86}Sr$ (Roveri, Lugli, et al., 2014), excluding a marine origin. There is moreover no faunal evidence for a marine salinity incursion in the Dacian Basin at the onset of the Bosphorian (Stoica et al., 2013). The high $^{87}Sr/^{86}Sr$ in the basal Bosphorian are therefore most likely derived from a Lake Pannon origin (Stoica et al., 2013). However, it seems hard to ascribe a water level rise in excess of 50 m together with an increase in salinity (inferred from ostracod assemblages; Stoica et al., 2013) solely to extra outflow of Lake Pannon waters. Such an explanation would also require the Dobrogea sill separating the Dacian basin from the Black Sea to be uplifted, and/or the Dacian Basin to experience increased subsidence (in which case the Lake Pannon would have an outflow into the isolated Dacian Basin), while the salinity increase suggests a connection to a more saline source. As alternative the increased salinity suggested by the faunal assemblages at the onset of the Bosphorian could also be explained by an isolated Lake Pannon-Dacian Basin system. In this case, Lake Pannon, presumably located at a higher elevation, would have been outflowing into the endorheic Dacian Basin, the latter being unable to export the solutes generated through evaporation, becoming increasingly saltier. Further elucidation of the mechanism and the exact timing of events characterizing the Bosphorian Flood require $^{87}Sr/^{86}Sr$ additional data of Lake Pannon during MSC times and more robust constraints on the paleoenvironmental changes in the Dacian Basin.

The principles of the strontium method argue that interconnected basins should have more or less the same $^{87}Sr/^{86}Sr$ (e.g., Flecker & Ellam, 2006). The $^{87}Sr/^{86}Sr$ of the Dacian Basin (>0.7088) and the Black Sea (0.7085–0.7086), however, differ significantly during the Messinian Salinity Crisis (Figure 7). This implies that the waters from the two basins were not fully mixed. The Dacian Basin was, however, not fully disconnected from the Black Sea, because some $^{87}Sr/^{86}Sr$ (reaching 0.708865 low at 5.58 Ma; Figure 7; Table 1) are below the lower limit of the Danube (<0.7089) and closer to the coeval Black Sea ones (Grothe et al., 2020; Figure 7). Remarkable is the opposite trends in the $^{87}Sr/^{86}Sr$ of Dacian Basin when compare to the Black Sea record. These converging $^{87}Sr/^{86}Sr$ trends hint for water exchange between Dacian Basin and Black Sea (Figure 7). We conclude that water exchange between the basins must have been subtle to maintain different strontium isotopic compositions in the basins. For example, the relatively narrow dimensions of the present-day Bosporus Strait are already sufficient for the Black Sea to have typical marine $^{87}Sr/^{86}Sr$ (Major et al., 2006). The gateway connecting the Dacian and Black Sea basins must, therefore, have had much smaller exchange dimensions than the present-day Bosporus Strait and/or must have been subject to very different hydrological fluxes. This is in contradiction with paleogeographical maps of the Pontian in

which the Eastern Paratethys Sea is often depicted as one large unified water mass (e.g., Popov et al., 2006; Figure 1).

7.4. The Zanclean Flood and the Early Pliocene

The Miocene-Pliocene boundary in the Mediterranean Basin is marked by a sharp transition from low-saline Lago Mare deposits during the latest Miocene to normal marine deposits during the Pliocene (e.g., Roveri, Flecker, et al., 2014). The return to normal marine conditions in the Mediterranean is described as the Zanclean Flood. This abrupt environmental shift is also reflected in the Mediterranean $^{87}Sr/^{86}Sr$ record, which evolves from relatively low restricted ratios to normal marine ratios in the earliest Pliocene (Figure 7; Roveri, Flecker, et al., 2014).

A similar increase to normal marine strontium isotope ratios is not observed in the Dacian Basin at the Miocene-Pliocene boundary (Figure 8). Instead, $^{87}Sr/^{86}Sr$ records a drop across this transition, suggesting that marine waters had not entered the Dacian Basin. This observation is in agreement with paleontological proxies indicating no marine influence at this time in the Dacian Basin and the Black Sea (Krijgsman et al., 2010; Stoica et al., 2013; Vasiliev et al., 2013; van Baak, Radionova, et al., 2015). Additionally, unlike the abrupt $^{87}Sr/^{86}Sr$ shift at the Zanclean Flood from Mediterranean, the Dacian Basin record shows a rather gradual decrease (Figure 7), verging towards a Black Sea-like $^{87}Sr/^{86}Sr$ during the Last Glacial Maximum (LGM; Major et al., 2006; Vasiliev et al., 2010). Remarkable is the also the opposing trends of the Dacian Basin and the other basins of the Eastern Paratethys (i.e., Caspian Basin) suggesting a unification of the Eastern Paratethys sub-basins (Figure 7).

Another important observation is that the $^{87}Sr/^{86}Sr$ of the Dacian Basin during the Pliocene are lower than those observed during the latest Messinian (Figures 5 and 7; Vasiliev et al., 2010). The Pliocene $^{87}Sr/^{86}Sr$ of the Dacian Basin are comparable to the Black Sea during the LGM (Major et al., 2006; Vasiliev et al., 2010) when the Black Sea was disconnected from the open ocean and fed by rivers draining the Russian Platform (e.g., Don, Dnieper, Dniester; more than during present-day) and the Danube. At this time, the Black Sea was also disconnected from the Caspian Sea, which experienced a dramatic lowstand during deposition of the so-called Productive Series (Abdullayev et al., 2012).

The early Pliocene $^{87}Sr/^{86}Sr$ of Slanicul de Buzau show similarity with the data from Rîmnicu Sărat (Vasiliev et al., 2010). As most of these ratios fall within the observed range for $^{87}Sr/^{86}Sr$ during the LGM, we concur with the conclusion of Vasiliev et al. (2010) that the Black Sea and Dacian Basin were interconnected at that time without an appreciable connection to the Mediterranean.

7.5. The Plescoi Flood

The Plescoi flooding event at ~3.1 Ma is most likely related to a highstand of the Black Sea during the middle Pliocene Warm Period (Van Baak, Mandic, et al., 2015). At this time, typical brackish Black Sea species are present in the Slanicul de Buzau section. It is unclear whether the Black Sea highstand is related to a global sea level rise or a regional switch towards a more positive hydrological budget. The latter scenario requires the Black Sea to be disconnected from the Mediterranean; otherwise surplus water would spill into the Mediterranean, without changing the water levels of the Black Sea (e.g., La Vara et al., 2016; Krijgsman et al., 2010).

The observed $^{87}Sr/^{86}Sr$ during the Plescoi flooding event (~0.7089) does not approach open ocean ratios (~0.70905; Figure 5). It is therefore unlikely that marine waters directly affected the Dacian Basin. A similar scenario to the Heinrich Stadial 1 events can be envisaged, meltwater floods were sourced from a Northern Baltic region (Yanchilina et al., 2019). These interpretations are in agreement with faunal studies suggesting that during this event the salinity approached only the lower part of the brackish spectrum (<10) (Van Baak, Mandic, et al., 2015).

8. Conclusions

Strontium isotopes ratios of Miocene-Pliocene ostracods were used to reconstruct the connectivity of the Dacian Basin between 7.6 and 1.7 Ma. Relatively elevated $^{87}Sr/^{86}Sr$ originated either from marine incursions from water supplied by the Balta delta in the East Carpathian Foreland, or from outflow waters of Lake Pannon and local rivers, while low $^{87}Sr/^{86}Sr$ likely originated from connectivity with the Black Sea region. High isotopic ratios during the early and late Maeotian likely relate to a high input of riverine water coming from the Balta delta. The subsequent late Maeotian transgression in the Dacian Basin, shows decreasing isotopic ratios indicating progressive mixing with waters coming from the Black Sea-base, suggesting a high base-water level. The Pontian Flood interval (ca. 6.1 Ma) is marked by highly fluctuating $^{87}Sr/^{86}Sr$ that are attributed to a connection with the Black Sea (first isotopic minimum), a marine incursion in Paratethys from the Mediterranean (first isotopic maximum), continuing connectivity with the Black Sea, where the marine influence had drastically diminished (second isotopic minimum) and finally increased influence of Lake Pannon outflow (second isotopic maximum). During the Pontian Stage, that is the MSC interval, relatively low $^{87}Sr/^{86}Sr$ (<0.7085) indicate an increased connection with the Black Sea. The $^{87}Sr/^{86}Sr$ of the Dacian Basin, however, differs from the Black and Caspian Seas, which indicates that a sill separated the two basins limiting water exchange. The Bosphorian transgression at ca. 5.5 Ma was probably related to the increased influence of Pannonian water in the Dacian Basin, following which $^{87}Sr/^{86}Sr$ in the Dacian Basin and the Caspian Basin display a trend of convergence, suggesting mixing. The Zanclean Flood at 5.33 Ma in the Mediterranean Basin did not reach the Dacian Basin. The Plescoi Flood event at ~3.1 Ma is not marked by marine $^{87}Sr/^{86}Sr$ and its nature is therefore not comparable to the Pontian Flood. When evaluating the application of $^{87}Sr/^{86}Sr$ in assessing the connectivity (i.e., to open ocean) we conclude that the Dacian Basin (between 7.6 and 1.7 Ma) is an opposite counterpart to the Mediterranean during the MSC. While the latter was a marine basin affected by relatively short term disconnection form the ocean, the former (the Dacian basin) was a part of a large brackish-lacustrine isolated domain affected by a very short connection to the marine realm.

Data Availability Statement

The data is stored in PANGAEA database (www.pangaea.de) under https://doi.pangaea.de/10.1594/PANGAEA.932842.

Acknowledgments
We thank R. Smeets, M. Klaver, L. Kootker, M. van der Ven for assistance in the strontium laboratory at the VU, Amsterdam. Further we thank L. de Nooijer, W. Boer and H. de Waard for assistance with the LA-ICPMS measurements at the NIOZ and the UU. This work was financially supported by the Netherlands Geosciences Foundation (ALW) with support from the Netherlands Organization for Scientific Research (NWO) through the VICI grant of WK, Fundação de Amparo à Pesquisa do Estado de São Paulo (FAPESP) through the grant 2018/20733-6 of DVP and the Romanian Research Council Young Research Teams (PN-II-RU-TE-2014-4-0050) grant of IV.

References

Abdullayev, N. R., Riley, G. W., & Bowman, A. P. (2012). Regional controls on Lacustrine sandstone reservoirs: The Pliocene of the South Caspian Basin. In O. W. Baganz, Y. Bartov, K. Bohacs, & D. Nummedal (Eds.), *Lacustrine sandstone reservoirs and hydrocarbon systems AAPG memoir 95* (p. 71–98). The American Association of Petroleum Geologists.

Andreetto, F., Aloisi, G., Raad, F., Heida, H., Flecker, R., Agiadi, K., et al. (2021). Freshening of the Mediterranean salt giant: Controversies and certainties around the terminal (Upper Gypsum and Lago-Mare) phases of the Messinian Salinity Crisis. *Earth-Science Reviews*, *216*, 103577. https://doi.org/10.1016/j.earscirev.2021.103577

Andreetto, F., Matsubara, K., Beets, C. J., Fortuin, A. R., Flecker, R., & Krijgsman, W. (2021). High Mediterranean water-level during the Lago-Mare phase of the Messinian Salinity Crisis: Insights from the Sr isotope records of Spanish marginal basins (SE Spain). *Palaeogeography, Palaeoclimatology, Palaeoecology*, *562*, 110139. https://doi.org/10.1016/j.palaeo.2020.110139

Bethoux, J. P., & Pierre, C. (1999). Mediterranean functioning and sapropel formation: Respective influences of climate and hydrological changes in the Atlantic and the Mediterranean. *Marine Geology*, *153*(1), 29–39. https://doi.org/10.1016/s0025-3227(98)00091-7

Buhl, D., Neuser, R. D., Richter, D. K., Riedel, D., Roberts, B., Strauss, H., Veizer, J., et al. (1991). Nature and nurture: Environmental isotope story of the River Rhine. *Naturwissenschaften*, *78*, 337–346. https://doi.org/10.1007/BF01131605

Chivas, A.R., De Deckker, P., & Shelley, J.M.G. (1985). Strontium content of ostracods indicates lacustrine palaeosalinity. *Nature*, *316*, 251–253.

Clauer, N., Chaudhuri, S., Toulkeridis, T., & Blanc, G. (2000). Fluctuations of Caspian sea level: Beyond climatic variations? *Geology*, *28*, 1015–1018. https://doi.org/10.1130/0091-7613(2000)028<1015:focslb>2.3.co;2

Cramp, A., & O'Sullivan, G. (1999). Neogene sapropels in the Mediterranean: A review. *Marine Geology*, *153*, 11–28. https://doi.org/10.1016/s0025-3227(98)00092-9

De Leeuw, A., Tulbure, M., Kuiper, K. F., Melinte-Dobrinescu, M. C., Stoica, M., & Krijgsman, W. (2018). New $^{40}Ar/^{39}Ar$, magnetostratigraphic and biostratigraphic constraints on the termination of the Badenian Salinity Crisis: Indications for tectonic improvement of basin interconnectivity in Southern Europe. *Global and Planetary Change*, *169*, 1–15. https://doi.org/10.1016/j.gloplacha.2018.07.001

De Leeuw, A., Vincent, S. J., Matoshko, A., Stoica, M., & Igorara, I. (2020). Late Miocene sediment delivery from the axial drainage system of the East Carpathian foreland basin to the Black Sea. *Geology*, *48*. https://doi.org/10.1130/G47318.1

Flecker, R., De Villiers, S., & Ellam, R. M. (2002). Modeling the effect of evaporation on the salinity $^{87}Sr/^{86}Sr$ relationship in modern and ancient marginal-marine systems: The Mediterranean Messinian Salinity Crisis. *Earth and Planetary Science Letters*, *203*, 221–233. https://doi.org/10.1016/s0012-821x(02)00848-8

Flecker, R., & Ellam, R. M. (2006). Identifying Late Miocene episodes of connection and isolation in the Mediterranean–Paratethyan realm using Sr isotopes. *Sedimentary Geology*, *188–189*, 189–203. https://doi.org/10.1016/j.sedgeo.2006.03.005

Flecker, R., Krijgsman, W., Capella, W., de Castro Martíns, C., Dmitrieva, E., Mayser, J. P., et al. (2015). Evolution of the late Miocene Mediterranean-Atlantic gateways and their impact on regional and global environmental change. *Earth-Science Reviews*, *150*, 365–392. https://doi.org/10.1016/j.earscirev.2015.08.007

Gliozzi, E., Ceci, M. E., Grossi, F., & Ligios, S. (2007). Paratethyan Ostracod immigrants in Italy during the Late Miocene. *Geobios*, *40*, 325–337. https://doi.org/10.1016/j.geobios.2006.10.004

Grothe, A., Andreetto, F., Reichart, G.-J., Wolthers, M., van Baak, C. G. C., Vasiliev, I., et al. (2020). Paratethys pacing of the Messinian Salinity Crisis: Low salinity waters contributing to gypsum precipitation? *Earth and Planetary Science Letters*, *532*, 116029. https://doi.org/10.1016/j.epsl.2019.116029

Grothe, A., Sangiorgi, F., Brinkhuis, H., Stoica, M., & Krijgsman, W. (2018). Dispersal of the dinoflagellate Galeacysta etrusca and its implications for the Messinian Salinity Crisis. *Newsletters on Stratigraphy*, *51*, 73–91. https://doi.org/10.1127/nos/2016/0340

Hilgen, F. J., Lourens, L. J., van Dam, J. A., Beu, A. G., Boyes, A. F., Cooper, R. A., et al. (2012). The Neogene period. In *The geologic time scale* (pp. 923–978). Elsevier. https://doi.org/10.1016/b978-0-444-59425-9.00029-9

Jipa, D., Mațenco, L., Olteanu, R., Poenaru, C., Radan, S.-C., & Olariu, C. (2009). *Dacian basin: Depositional architecture and sedimentary history of a Paratethys Sea*. National Institute of Marine Geology and Geo-ecology (GeoEcoMar).

Jochum, K. P., Weis, U., Stoll, B., Kuzmin, D., Yang, Q., Raczek, I., et al. (2011). Determination of reference values for NIST SRM 610-617 glasses following ISO guidelines. *Geostandards and Geoanalytical Research*, *35*, 397–429. https://doi.org/10.1111/j.1751-908x.2011.00120.x

Jorissen, E., Abels, H., Wesselingh, F., Lazarev, S., Aghayeva, V., & Krijgsman, W. (2020). Amplitude, frequency and drivers of Caspian Sea lake-level variations during the Early Pleistocene and their impact on a protected wave-dominated coastline. *Sedimentology*, *67*, 649–676. https://doi.org/10.1111/sed.12658

Jorissen, E. L., De Leeuw, A., van Baak Ch, G. C., Mandic, O., Stoica, M., Abels, H. A., & Krijgsman, W. (2018). Sedimentary architecture and depositional controls of a Pliocene river-dominated delta in the semi-isolated Dacian Basin. *Sedimentary Geology*, *368*, 1–23. https://doi.org/10.1016/j.sedgeo.2018.03.001

Karami, M. P., Leeuw, A. D., Krijgsman, W., Meijer, P. T., & Wortel, M. J. R. (2011). The role of gateways in the evolution of temperature and salinity of semi-enclosed basins: An oceanic box model for the Miocene Mediterranean Sea and Paratethys. *Global and Planetary Change*, *79*, 73–88. https://doi.org/10.1016/j.gloplacha.2011.07.011

Kober, B., Schwalb, A., Schettler, G., & Wessels, M. (2007). Constraints on paleowater dissolved loads and on catchment weathering over the past 16 ka from $^{87}Sr/^{86}Sr$ ratios and Ca/Mg/Sr chemistry of freshwater ostracode tests in sediments of Lake Constance, Central Europe. *Chemical Geology*, *240*, 361–376. https://doi.org/10.1016/j.chemgeo.2007.03.005

Krijgsman, W., Capella, W., Simon, D., Hilgen, F. J., Kouwenhoven, T. J., Th, P., et al. (2018). The gibraltar corridor: Watergate of the Messinian salinity crisis. *Marine Geology*, *403*, 238–246. https://doi.org/10.1016/j.margeo.2018.06.008

Krijgsman, W., Stoica, M., Vasiliev, I., & Popov, V. V. (2010). Rise and fall of the Paratethys Sea during the Messinian Salinity Crisis. *Earth and Planetary Science Letters*, *290*, 183–191. https://doi.org/10.1016/j.epsl.2009.12.020

Kuhlemann, J. (2007). Paleogeographic and paleotopographic evolution of the Swiss and Eastern Alps since the Oligocene. *Global and Planetary Change*, *58*(1–4), 224–236. https://doi.org/10.1016/j.gloplacha.2007.03.007

La Vara, A., de van Baak, C. G. C., Marzocchi, A., Grothe, A., & Meijer, P. T. (2016). Quantitative analysis of Paratethys sea level change during the Messinian Salinity Crisis. *Marine Geology*, *379*, 39–51. https://doi.org/10.1016/j.margeo.2016.05.002

Lazarev, S., de LeeuwStoica, A. M., Mandic, O., van Baak, C. G. C., Vasiliev, I., & Krijgsman, W. (2020). From Khersonian drying to Pontian "flooding": Late Miocene stratigraphy and palaeoenvironmental evolution of the Dacian Basin (Eastern Paratethys). *Global and Planetary Change*, *192*, 103224. https://doi.org/10.1016/j.gloplacha.2020.103224

Magyar, I., & Geary, & D. H. (2012). Biostratigraphy in a Late Neogene Caspian-Type Lacustrine Basin: Lake Pannon, Hungary. Lacustrine Sandstone Reservoirs and Hydrocarbon Systems, *AAPG Memoire*, 95, 255–264. https://doi.org/10.1306/13291392M953142

Magyar, I., Geary, D. H., & Müller, P. (1999). Paleogeographic evolution of the Late Miocene Lake Pannon in Central Europe. *Palaeogeography, Palaeoclimatology, Palaeoecology*, *147*, 151–167. https://doi.org/10.1016/S0031-0182(98)00155-2

Magyar, I., Krezsek, C., & Tari, G. (2019). Clinoforms as paleogeographic tools: Development of the Danube catchment above the deep Paratethyan basins in central and southeast Europe. *Basin Research*, *32*, 320–331. https://doi.org/10.1111/bre.12401

Major, C. O., Goldstein, S. L., Ryan, W. B. F., Lericolais, G., Piotrowski, A. M., & Hajdas, I. (2006). The co-evolution of Black Sea level and composition through the last degla-ciation and its paleoclimatic significance. *Quaternary Science Reviews*, *25*, 2031–2047. https://doi.org/10.1016/j.quascirev.2006.01.032

Marunțeanu, M., & Papaianopol, I. (1995). The connection between the Dacic and Mediterranean Basins based on calcareous nannoplankton assemblages. *Romanian Journal of Stratigraphy*, *76*, 169–170.

Mason, P. R. D., & Kraan, W. J. (2002). Attenuation of spectral interferences during laser ablation inductively coupled plasma mass spectrometry (LA-ICP-MS) using an rf only collision and reaction cell. *Journal of Analytical Atomic Spectrometry*, *17*, 858–867. https://doi.org/10.1039/b202964b

Mațenco, L., Bertotti, G., Cloetingh, S., & Dinu, C. (2003). Subsidence analysis and tectonic evolution of the external Carpathian–Moesian Platform region during Neogene times. *Sedimentary Geology*, *156*, 71–94. https://doi.org/10.1016/S0037-0738(02)00283-X

Matoshko, A., Matoshko, A., De Leeuw, A., & Stoica, M. (2016). Facies analysis of the Balta Formation: Evidence for a large late Miocene fluvio deltaic system in the East Carpathian foreland. *Sedimentary Geology*, *343*, 165–189. https://doi.org/10.1016/j.sedgeo.2016.08.004

McArthur, J. M., Howarth, R. J., & Shields, G. A. (2012). Strontium isotope stratigraphy. In F. M. Gradsteini, J. G. Ogg, M. Schmitz, & G. Ogg (Eds.), *The geologic timescale* (pp. 127–144). Elsevier. https://doi.org/10.1016/B978-0-444-59425-9.00007-X

McCulloch & De Deckker (1989). Sr isotope constraints on the Mediterranean environment at the end of the Messinian salinity crisis. *Nature*, *342*, 62–65. https://doi.org/10.1038/342062a0

Miklós, D., & Neppel, F. (2010). In M. Brilly (Ed.), *Hydrological processes of the Danube River basin: Perspectives from the danubian countries* (pp. 79–124). Springer Netherlands. https://doi.org/10.1007/978-90-481-3423-6_3

Motas, I., Bandrabur, T., Ghenea, C., & Sandulescu, M. (1966). *Geologic map of Romania: 1:200 000, ploiesti sheet*.

Munteanu, I., Mațenco, L., Dinu, C., & Cloetingh, S. (2012). Effects of large sea-level variations in connected basins: The Dacian-Black Sea system of the Eastern Paratethys. *Basin Research*, *24*(5), 583–597. https://doi.org/10.1111/j.1365-2117.2012.00541.x

Olariu, C., Jipa, D., & Krézsek, C. (2018). The Danube River inception: Evidence for a 4 Ma continental-scale river born from segmented Paratethys basins. *Terra Nova*, *30*, 63–71. https://doi.org/10.1111/ter.12308

Palcu, D. V., Vasiliev, I., Stoica, M., & Krijgsman, W. (2019). The end of the Great Khersonian Drying of Eurasia: Magnetostratigraphic dating of the Maeotian transgression in the Eastern Paratethys. *Basin Research*, *31*, 33–58. https://doi.org/10.1111/bre.12307

Palmer, M. R., & Edmond, J. M. (1992). The strontium isotope budget of the modern ocean. *Earth and Planetary Science Letters*, *92*, 11–26.
Pană, I., Bönig, N., & Botez, R. (1968). *New Elements in the Levantin Fauna in the Buzau Region (In Romanian)* (Vol. XDX, pp. 699–701). Petrol si Gaze.
Panaiotu, C. E., Vasiliev, I., Panaiotu, C. G., Krijgsman, W., & Langereis, C. G. (2007). Provenance analysis as a key to orogenic exhumation: A case study from the East Carpathians (Romania). *Terra Nova*, *19*, 120–126. https://doi.org/10.1111/j.1365-3121.2006.00726.x
Pawellekl, F., Frauenstein, F., & Veizer, J. (2002). Hydrochemistry and isotope geochemistry of the upper Danube River. *Geochimica et Cosmochimica Acta*, *66*(21), 3839–3854. https://doi.org/10.1016/S0016-7037(01)00880-8
Popov, S. V., Shcherba, I. G., Ilyina, L. B., Nevesskaya, L. A., Paramonova, N. P., Khondkarian, S. O., et al. (2006). Late Miocene to Pliocene paleogeography of the Paratethys and its relation to the Mediterranean. *Palaeogeography, Palaeoclimatology, Palaeoecology*, *238*, 91–106. https://doi.org/10.1016/j.palaeo.2006.03.020
Reghizzi, M., Gennari, R., Douville, E., Lugli, S., Manzi, V., Montagna, et al. (2017). Isotope stratigraphy ($^{87}Sr/^{86}Sr$, $\delta^{18}O$, $\delta^{13}C$) of the Sorbas basin (Betic Cordillera, Spain): Paleoceanographic evolution across the onset of the Messinian salinity crisis. *Palaeogeography, Palaeoclimatology, Palaeoecology*, *469*, 60–73. https://doi.org/10.1016/j.palaeo.2016.12.039
Reghizzi, M., Lugli, S., Manzi, F. P., & Roveri, M. (2018). Forced hydrological balance during the Messinian salinity crisis: Insights from strontium isotopes ($^{87}Sr/^{86}Sr$) in the Vena del Gesso Basin (Northern Apennines, Italy). *Paleoceanography and Paleoclimatology*, *33*, 716–731. https://doi.org/10.1029/2018pa003395
Roveri, M., Flecker, R., Krijgsman, W., Lofi, J., Lugli, S., Manzi, V., et al. (2014). The Messinian salinity crisis: Past and future of a great challenge for marine sciences. *Marine Geology*, *352*, 25–58. https://doi.org/10.1016/j.margeo.2014.02.002
Roveri, M., Lugli, S., Manzi, V., Gennari, R., & Schreiber, B. C. (2014). High-resolution strontium isotope stratigraphy of the Messinian deep Mediterranean basins: Implications for marginal to central basins correlation. *Marine Geology*, *349*, 113–125. https://doi.org/10.1016/j.margeo.2014.01.002
Schildgen, T. F., Cosentino, D., Frijia, G., Castorina, F., Dudas, F. Ö., Iadanza, A., & et al. (2014). Sea level and climate forcing of the Sr isotope composition of late Miocene Mediterranean marine basins. *Geochemistry, Geophysics, Geosystems*, *15*, 2964–2983. https://doi.org/10.1002/2014GC005332
Simon, D., Palcu, D., Meijer, P., & Krijgsman, W. (2019). The sensitivity of middle Miocene paleoenvironments to changing marine gateways in Central Europe. *Geology*, *47*, 35–38. https://doi.org/10.1130/G45698.1
Stevanovic, P., Nevesskaya, L.A., Marinescu, F., Sokac, A. & Jámbor, A. (Eds.). (1989). *Neogen der Westlichen („Zentralen") Paratethys, Pontien*. JAZU & SANU.
Stoica, M., Krijgsman, W., Fortuin, A., & Gliozzi, E. (2016). Paratethyan ostracods in the Spanish Lago-Mare: More evidence for interbasinal exchange at high Mediterranean sea level. *Palaeogeography, Palaeoclimatology, Palaeoecology*, *441*, 854–870. https://doi.org/10.1016/j.palaeo.2015.10.034
Stoica, M., Lazăr, I., Krijgsman, W., Vasiliev, I., Jipa, D., & Floroiu, A. (2013). Paleoenvironmental evolution of the East Carpathian foredeep during the late Miocene–early Pliocene (Dacian Basin; Romania). *Global and Planetary Change*, *103*, 135–148. https://doi.org/10.1016/j.gloplacha.2012.04.004
Topper, R. P. M., Flecker, R., Meijer, P. T., & Wortel, M. J. R. (2011). A box model of the Late Miocene Mediterranean Sea: Implications from combined $^{87}Sr/^{86}Sr$ and salinity data. *Paleoceanography*, *26*, PA3223. https://doi.org/10.1029/2010pa002063
van Baak, C. G. C., Krijgsman, W., Magyar, I., Sztanó, O., Golovina, L. A., Grothe, A., et al. (2017). Paratethys response to the Messinian salinity crisis. *Earth-Science Reviews*, *172*, 193–223. https://doi.org/10.1016/j.earscirev.2017.07.015
van Baak, C. G. C., Mandic, O., Lazar, I., Stoica, M., & Krijgsman, W. (2015). The Slanicul de Buzau section, a unit stratotype for the Romanian stage of the Dacian Basin (Plio- Pleistocene, Eastern Paratethys). *Palaeogeography, Palaeoclimatology, Palaeoecology*, *440*, 594–613. https://doi.org/10.1016/j.palaeo.2015.09.022
van Baak, C. G. C., Radionova, E. P., Golovina, L. A., Raffi, I., Kuiper, K. F., Vasiliev, I., et al. (2015). Messinian events in the Black Sea. *Terra Nova*, *27*, 433–441. https://doi.org/10.1111/ter.12177
Vasiliev, I., Iosifidi, A. G., Khramov, A. N., Krijgsman, W., Kuiper, K., Langereis, C. G., et al. (2011). Magnetostratigraphy and radio-isotope dating of upper Miocene - Lower Pliocene sedimentary successions of the Black Sea Basin (Taman Peninsula, Russia). *Palaeogeography, Palaeoclimatology, Palaeoecology*, *310*(3–4), 163–175. https://doi.org/10.1016/j.palaeo.2011.06.022
Vasiliev, I., Krijgsman, W., Langereis, C. G., Panaiotu, C. E., Maţenco, L., & Bertotti, G. (2004). Towards an astrochronological framework for the eastern Paratethys Mio–Pliocene sedimentary sequences of the Focşani basin (Romania). *Earth and Planetary Science Letters*, *227*, 231–247. https://doi.org/10.1016/j.epsl.2004.09.012
Vasiliev, I., Reichart, G.-J., Davies, G. R., Krijgsman, W., & Stoica, M. (2010). Strontium isotope ratios of the Eastern Paratethys during the Mio-Pliocene transition; implications for interbasinal connectivity. *Earth and Planetary Science Letters*, *292*, 123–131. https://doi.org/10.1016/j.epsl.2010.01.027
Vasiliev, I., Reichart, G.-J., & Krijgsman, W. (2013). Impact of the Messinian Salinity Crisis on Black Sea hydrology-insights from hydrogen isotopes analysis on biomarkers. *Earth and Planetary Science Letters*, *362*, 272–282. https://doi.org/10.1016/j.epsl.2012.11.038
Vonhof, H. B., Wesselingh, F. P., Guerrero, J., Kaandorp, R. J. G., Davies, G. R., van Hinte, J. E., et al. (2003). Paleogeography of Miocene Western Amazonia: Isotopic composition of molluscan shells constrains the influence of marine incursions. *Geological Society of America Bulletin*, *115*(8), 983–993. https://doi.org/10.1130/b25058.1
Yanchilina, A. G., RyanKenna, W. B. F. T. C., & McManus, J. F. (2019). Meltwater floods into the Black and Caspian Seas during Heinrich Stadial 1. *Earth-Science Reviews*, *198*, 102931. https://doi.org/10.1016/j.earscirev.2019.102931
Zitek, A., Tchaikovsky, A., Irrgeher, J., & Waidbacher, H. (2015). The 87Sr/86Sr river water isoscape of the Danube catchment: Joint Danube Survey 3: *A comprehensive Analysis of Danube Water Quality*, September, p. 349–344.